

# **SANDIA REPORT**

SAND2010-6173

Unlimited Release

September, 2010

## **Enhanced Performance Assessment System (EPAS) for Carbon Sequestration**

Yifeng Wang, Thomas Dewers, Teklu Hadgu, Carlos F. Jove-Colon, Amy C. Sun, and  
Jerry McNeish

Prepared by  
Sandia National Laboratories  
Albuquerque, New Mexico 87185 and Livermore, California 94550

Sandia is a multiprogram laboratory operated by Sandia Corporation,  
a Lockheed Martin Company, for the United States Department of Energy's  
National Nuclear Security Administration under Contract DE-AC04-94AL85000.

Approved for public release; further dissemination unlimited.

Issued by Sandia National Laboratories, operated for the United States Department of Energy by Sandia Corporation.

**NOTICE:** This report was prepared as an account of work sponsored by an agency of the United States Government. Neither the United States Government, nor any agency thereof, nor any of their employees, nor any of their contractors, subcontractors, or their employees, make any warranty, express or implied, or assume any legal liability or responsibility for the accuracy, completeness, or usefulness of any information, apparatus, product, or process disclosed, or represent that its use would not infringe privately owned rights. Reference herein to any specific commercial product, process, or service by trade name, trademark, manufacturer, or otherwise, does not necessarily constitute or imply its endorsement, recommendation, or favoring by the United States Government, any agency thereof, or any of their contractors or subcontractors. The views and opinions expressed herein do not necessarily state or reflect those of the United States Government, any agency thereof, or any of their contractors.

Printed in the United States of America. This report has been reproduced directly from the best available copy.

Available to DOE and DOE contractors from  
U.S. Department of Energy  
Office of Scientific and Technical Information  
P.O. Box 62  
Oak Ridge, TN 37831

Telephone: (865) 576-8401  
Facsimile: (865) 576-5728  
E-Mail: [reports@adonis.osti.gov](mailto:reports@adonis.osti.gov)  
Online ordering: <http://www.osti.gov/bridge>

Available to the public from  
U. S. Department of Commerce  
National Technical Information Service  
5285 Port Royal Rd.  
Springfield, VA 22161

Telephone: (800) 553-6847  
Facsimile: (703) 605-6900  
E-Mail: [orders@ntis.fedworld.gov](mailto:orders@ntis.fedworld.gov)  
Online order: <http://www.ntis.gov/help/ordermethods.asp?loc=7-4-0#online>



# Enhanced Performance Assessment System (EPAS) for Carbon Sequestration

Yifeng Wang<sup>1</sup>, Thomas Dewers<sup>1</sup>, Teklu Hadgu<sup>1</sup>, Carlos F. Jove-Colon<sup>1</sup>, Amy C. Sun<sup>1</sup>, and Jerry McNeish<sup>2</sup>

<sup>1</sup>Sandia National Laboratories  
P.O. Box 5800  
Albuquerque, New Mexico 87185

<sup>2</sup>Sandia National Laboratories  
7011 East Avenue  
Livermore, CA 94551

## Abstract

Carbon capture and sequestration (CCS) is an option to mitigate impacts of atmospheric carbon emission. Numerous factors are important in determining the overall effectiveness of long-term geologic storage of carbon, including leakage rates, volume of storage available, and system costs. Recent efforts have been made to apply an existing probabilistic performance assessment (PA) methodology developed for deep nuclear waste geologic repositories to evaluate the effectiveness of subsurface carbon storage (Viswanathan et al., 2008; Stauffer et al., 2009). However, to address the most pressing management, regulatory, and scientific concerns with subsurface carbon storage (CS), the existing PA methodology and tools must be enhanced and upgraded. For example, in the evaluation of a nuclear waste repository, a PA model is essentially a forward model that samples input parameters and runs multiple realizations to estimate future consequences and determine important parameters driving the system performance. In the CS evaluation, however, a PA model must be able to run both forward and inverse calculations to support optimization of CO<sub>2</sub> injection and real-time site monitoring as an integral part of the system design and operation. The monitoring data must be continually fused into the PA model through model inversion and parameter estimation. Model calculations will in turn guide the design of optimal monitoring and carbon-injection strategies (e.g., in terms of monitoring techniques, locations, and time intervals).

Under the support of Laboratory-Directed Research & Development (LDRD), a late-start LDRD project was initiated in June of Fiscal Year 2010 to explore the concept of an enhanced performance assessment system (EPAS) for carbon sequestration and storage. In spite of the tight time constraints, significant progress has been made on the project:

- (1) Following the general PA methodology, a preliminary Feature, Event, and Process (FEP) analysis was performed for a hypothetical CS system. Through this FEP analysis, relevant scenarios for CO<sub>2</sub> release were defined.
- (2) A prototype of EPAS was developed by wrapping an existing multi-phase, multi-component reservoir simulator (TOUGH2) with an uncertainty quantification and optimization code (DAKOTA).
- (3) For demonstration, a probabilistic PA analysis was successfully performed for a hypothetical CS system based on an existing project in a brine-bearing sandstone. The work lays the foundation for the development of a new generation of PA tools for effective management of CS activities.

At a top-level, the work supports energy security and climate change/adaptation by furthering the capability to effectively manage proposed carbon capture and sequestration activities (both research and development as well as operational), and it greatly enhances the technical capability to address this national problem.

The next phase of the work will include (1) full capability demonstration of the EPAS, especially for data fusion, carbon storage system optimization, and process optimization of CO<sub>2</sub> injection, and (2) application of the EPAS to actual carbon storage systems.

## **ACKNOWLEDGMENTS**

This work was supported by the Sandia National Laboratory Lab Directed Research and Development program , Project No. 150632. The authors appreciate the comments received during the development of the proposal from the LDRD office, and the conduct of the research. The report benefitted from the technical review provided by Clifford Hansen, and David Borns.

# CONTENTS

1. INTRODUCTION .....	10
2. CONCEPT OF ENHANCED PERFORMANCE ASSESSMENT SYSTEM (EPAS) .....	12
3. FEP ANALYSIS AND SCENARIO DEVELOPMENT .....	17
3.1. Hypothetical Carbon Sequestration System .....	17
3.2. Evaluation of FEPs .....	18
3.3. Scenario Description .....	26
4. DEVELOPMENT OF PROTOTYPE EPAS .....	28
4.1. Description of TOUGH2 .....	28
4.2. Description of DAKOTA .....	28
4.3. Wrapping TOUGH2 with DAKOTA .....	28
4.4. Parallel Version of DAKOTA-TOUGH2 .....	29
5. DEMONSTRATION OF PROTOTYPE EPAS .....	31
5.1. General Description of the Model .....	31
5.2. General Attributes of the Model .....	33
5.3. Results of EPAS demonstration .....	37
5.3.1. Deterministic case .....	37
5.3.2. Multiple realization case .....	41
5.4. Uncertainty Quantification and Sensitivity Analysis .....	46
6. DESCRIPTION OF OPTIMIZATION APPROACH .....	56
6.1. Selection of Optimization Metrics .....	56
6.2. Detailed Optimization of Carbon Sequestration System .....	56
6.3. Fusion of Modeling with Carbon Data .....	57
6.4. Management Tools for Prioritization of Carbon Sequestration Program .....	57
7. SUMMARY AND FOLLOW-ON WORK .....	58
8. REFERENCES .....	60
Distribution .....	63

## FIGURES

Figure 1. Conceptual diagram of CO <sub>2</sub> sequestration (WRI, 2010) .....	10
Figure 2. Enhanced Approach to Performance Assessment of Carbon Storage .....	14
Figure 3. Enhanced Performance Assessment System (EPAS) Architecture .....	15
Figure 4. Schematic of Modeled System .....	17
Figure 5. Schematic of DAKOTA-based EPAS framework .....	29
Figure 6. Schematic of hybrid parallelism used in the CSS-PA study .....	30
Figure 7. Conceptual reservoir-caprock-aquifer model for subsurface carbon storage, with superimposed numerical grid for TOUGH2 simulations. ....	33
Figure 8. A. Capillary pressure curves for “Clean” and “Shaly” Frio Formation sands showing select data points from Holtz et al. (2005) and corresponding fit to van Genuchten formation. B. Corresponding gas and liquid relative permeability for the upper Frio “Clean” sand plotted as a function of liquid, or brine, saturation. C. Capillary pressure function for Anahuac Formation shale, via select data points, and corresponding fit to van Genuchten formulation. D. Gas and liquid relative permeability for Anahuac Formation as determined using capillary pressure curve parameters. ....	35
Figure 9. Frequency distributions of porosity and permeability used in 20 TOUGH2 material properties. ....	36
Figure 10. Mesh, location of injection and leaky wells, FOFT cells, and spatial heterogeneity in porosity and permeability in the storage reservoir. ....	37
Figure 11. Profiles with time of consequences of CO <sub>2</sub> injection using the mesh and model shown in Figure 7. A. Profiles of pressure (Pa) after 1, 5, 10, and 50 years of injection. B. Profiles of scCO <sub>2</sub> saturation after 1, 5, 10, and 50 years. C. Profiles of mass fraction of NaCl (both dissolved in aqueous solution and solid) after 1, 5, 10, and 50 years. The high NaCl amounts near the injection well are solid salt, due to dry-out associated with injection near the wellbore. D. Profiles of aqueous CO <sub>2</sub> after 1, 5, 10, and 50 years of injection. ....	40
Figure 12. Time series of pressure, scCO <sub>2</sub> saturation, aqueous CO <sub>2</sub> and mass fraction of NaCl for elements 2121 and 3551 in the TOUGH2 grid. Element 2121 occurs just above the injection well at the reservoir caprock boundary, while element 3551 occurs just above the injection well at the caprock-aquifer boundary. ....	41
Figure 13. Pressure in Injection Well (Element 821) –27 Vectors .....	43
Figure 14. Gas Saturation in Injection Well (Element 821) –27 Vectors .....	43
Figure 15. Pressure in Abandoned Well (Element 1782) –27 Vectors. Discrete appearance of the curves are due to the limited number of model output data points. ....	44
Figure 16. Gas Saturation in Abandoned Well (Element 1782) – 27 Vectors .....	44
Figure 17. CO <sub>2</sub> Leakage from Abandoned Well (Element 1782) – 27 Vectors .....	45
Figure 18. Gas Flowrate at the Reservoir-Caprock Boundary (Element 1991 to Element 2121) – 27 Vectors. (Negative flowrate indicates flow from reservoir to caprock) .....	45
Figure 19. Gas Flowrate at the Caprock-Aquifer Boundary (Element 3421 to Element 3551) – 27 Vectors. (Negative flowrate indicates flow from caprock to aquifer) .....	46
Figure 20. Total amount of carbon dioxide in gas phase within the overlying aquifer after 100 years. ....	47
Figure 21. Total amount of dissolved carbon dioxide in aqueous phase within the overlying aquifer after 100 years. ....	47

Figure 22. Total amount of carbon dioxide in gas phase within caprock after 100 years .....	48
Figure 23. Total amount of dissolved carbon dioxide in aqueous phase within caprock after 100 years. ....	48
Figure 24. Total amount carbon dioxide in gas phase within reservoir after 100 years. ....	49
Figure 25. Total amount of dissolved carbon dioxide in aqueous phase within reservoir after 100 years. ....	50
Figure 26. Sampled porosity values versus total dissolved CO <sub>2</sub> within the reservoir after 100 years. ....	51
Figure 27. Sampled permeability values versus total dissolved CO <sub>2</sub> within the reservoir after 100 years. ....	51
Figure 28. Sampled residual water saturation versus total dissolved CO <sub>2</sub> within the reservoir after 100 years. ....	52
Figure 29. Sampled injection rates versus total dissolved CO <sub>2</sub> within the reservoir after 100 years. ....	52
Figure 30. Sampled productivity indices versus total dissolved CO <sub>2</sub> within the reservoir after 100 years. ....	53
Figure 31. Sampled porosity values versus total gas-phase CO <sub>2</sub> within the reservoir after 100 years. ....	53
Figure 32. Sampled permeability values versus total gas-phase CO <sub>2</sub> within the reservoir after 100 years. ....	54
Figure 33. Sampled residual water saturation versus total gas-phase CO <sub>2</sub> within the reservoir after 100 years. ....	54
Figure 34. Sampled injection rates versus total gas-phase CO <sub>2</sub> within the reservoir after 100 years. ....	55
Figure 35. Sampled productivity indices versus total gas-phase CO <sub>2</sub> within the reservoir after 100 years. ....	55
Figure 36. Map of Carbon Sequestration Projects in U.S. (NETL, 2010b) .....	57

## TABLES

Table 1. FEP Analysis.....	18
Table 2. Sequestration Scenarios .....	27
Table 3. List of Input Parameters .....	31
Table 4. Petrophysical parameters for the upper Frio Formation and Anahuac Formation shale (after Holtz et al., 2005) .....	34
Table 5. Summary of Follow-on Work to Further this Research .....	59



## ACRONYMS

CS	Carbon storage
CCS	Carbon capture and storage
DOE	Department of Energy
EPAS	Enhanced Performance Assessment System
FEP	Feature, event, process
PA	Performance Assessment
SNL	Sandia National Laboratories
UQ	Uncertainty quantification
V&V	Verification and validation



integral part of the system design and operation. The monitoring data must be continually fused into the PA model through model inversion and parameter estimation. Model calculations will in turn guide the design of optimal monitoring and carbon-injection strategies (e.g., in terms of monitoring techniques, locations, and time intervals).

Under the support of Laboratory-Directed Research & Development (LDRD), a late-start LDRD project was initiated in fiscal year 2010 to explore the concept of an enhanced performance assessment system (EPAS) for carbon sequestration and storage. This report documents the results of this project obtained to date. The remaining sections of the document are as follows:

- Section 2 describes the concept of the enhanced performance assessment system (EPAS), with both a forward modeling and an inverse modeling structure. The inverse modeling structure has been defined, and prototyped with software linkage in this document, but not significantly exercised.
- Section 3 documents the review of the features, events and processes that are applicable to the evaluation of subsurface carbon storage. Preliminary scenarios for evaluation of such systems are identified.
- Section 4 provides the overall structure of the prototype EPAS, with a description of the two major softwares used in this evaluation, DAKOTA and TOUGH2. The conceptual depiction of the linkage of the codes provides a high level understanding of the important aspects of this type of analysis, and points to the future application in a high-performance computational platform for analysis of such complex systems.
- Section 5 presents the demonstration of the prototype EPAS case conducted in this LDRD. The parameters for the model, both deterministic and uncertain, are provided. The general overall results for the simulated case are also provided, with some discussion of their importance. A brief discussion of uncertainty quantification and sensitivity analysis is also provided. This aspect of the EPAS structure is expected to be exercised significantly in future work.
- Section 6 provides a brief roadmap to the optimization approach that can be conducted utilizing the EPAS approach, specifically focusing on the subsurface carbon storage application.
- Section 7 lists a brief summary of the work conducted thus far on EPAS, and potential additional aspects of the modeling effort that can be further developed.
- Finally, Section 8 provides the references for the report.

## 2. CONCEPT OF ENHANCED PERFORMANCE ASSESSMENT SYSTEM (EPAS)

A probabilistic performance assessment (PA) of a geologic repository was originally developed for nuclear waste disposal. In that arena, a PA intends to provide the stakeholders with an analysis of disposal system performance. A PA analysis is designed to answer four key questions related to the waste isolation capability of a nuclear waste disposal system (Helton, et al., 1999):

- I. Scenario identification - What can happen?
- II. Likelihood of scenarios – How likely is it to happen?
- III. Consequences of scenarios – What are the consequences if it does happen?
- IV. Credibility – How much confidence do we have in the answers to the first three questions?

The performance of a disposal system is generally described with pre-defined regulatory metrics; for example, the peak dose or cumulative dose that a hypothetical receptor can potentially be exposed to within a regulatory time, typically ranging from 10,000 to 1 million years. The release dose is calculated by accounting for the release rates of all radionuclides at a specified disposal system boundary, the dilution factor, and the toxicity of radionuclides. In a license application, the licensee is required to compare the projected dose with a standard set up by a regulatory agency. The safety margin of a disposal system is defined as the difference between the regulatory standard and the projected value of the performance metrics. A licensee is also generally required to provide the uncertainty – the confidence – associated with the projected safety margin. The safety margin analysis and uncertainty quantification are thus an integral part of the performance assessment of a nuclear waste disposal system. It is generally believed that the PA methodology could be extended to evaluate the performance of a CS system.

Some effort has been made to use probabilistic risk analysis methods to assess the potential failure of CS systems (e.g., leakage; Walton et al. 2005; Rish 2005) or to evaluate CO<sub>2</sub> retention performance and economic issues (Viswanathan et al. 2008; LeNeveu 2008; Burruss et al. 2009; Oldenburg et al. 2009; and Stauffer et al. 2009). The work of Viswanathan et al. (2008) and Stauffer et al. (2009) is the most relevant to our current approach of system modeling. Their model, CO<sub>2</sub>-PENS, analyzes CO<sub>2</sub> injection and trapping in the reservoir along with economics by adopting probability methodologies to characterize uncertainty in their simulations. CO<sub>2</sub>-PENS is defined by process-level modules that are coupled together using the Goldsim<sup>®</sup> software package (GoldSim, 2010) to capture all pertinent stages of CO<sub>2</sub> sequestration from gas generation at the plant to injection into the target reservoir. This model makes use of a ‘reduced complexity injection function’ that takes the form of an analytical solution to compute CO<sub>2</sub> injection into a reservoir. The authors indicate that the analytical solution, albeit considerably simplified, can represent the linear behavior of reservoir properties such as porosity and permeability for a specified injection pressure, relative permeability, pressure and temperature. The analytical solution is ‘tuned’ to represent the general trends obtained by a fully coupled injection flow model. The ‘tuning’ of the reduced complexity analytical solution is done by slope regression using 2-D radial calculations from the LANL multiphase porous flow code

FEHM (Stauffer et al. 2009). The main advantage of using a reduced complexity approach is to greatly decrease the amount of time needed to execute the simulations. However, Stauffer et al. (2009) recognize that such an approach cannot capture the details of a fully coupled flow model. Moreover, the authors note that the main intent of the model is to provide initial scoping calculations to estimate important quantities such as reservoir capacity in the evaluation of site selection. For the PA of a specific site with well-established reservoir properties, then the module can be substituted with one that can perform more complex multiphase flow calculations (Stauffer et al. 2009). The authors also note that although the reduced complexity approach can produce results in ~40 minutes (5000 realizations), the same problem using the FEHM flow simulator would take ~3 days to complete. In addition, the capability of the FEHM for capturing supercritical CO<sub>2</sub> behavior still needs to be demonstrated.

In this report we attempt to formulate the enhanced PA concept for CS systems and establish a prototype framework for this concept. The flow chart for the enhanced approach is shown in Figure 2. The forward model components represent the typical steps of the existing PA methodology. According to the existing methodology, a PA starts with Feature, Event, and Process (FEP) evaluation, through which potentially important FEPs are identified for inclusion for further PA analysis. FEP evaluation also helps define performance scenarios of a CS system of interest by identifying major CO<sub>2</sub> release pathways. The next step of a PA analysis is to develop appropriate computational models for the selected FEPs and the defined performance scenarios and then to constrain model input parameters. The model input parameter values and their uncertainty distributions are constrained from field observations and laboratory experimental data. The whole cycle of a PA analysis is then completed by uncertainty quantification and sensitivity analysis, typically performed using multiple Monte-Carlo simulations. The whole PA process is generally iterative. EPAS extends the existing PA methodology by adding the inverse model components, as shown in Figure 2. These inverse components provide necessary tools for optimization of long-term system performance, process optimization of CO<sub>2</sub> injection, as well as updating of parameter estimates as new data are obtained. To fulfill these new functionalities, the EPAS must have a built-in optimization capability. The new PA framework includes a built-in optimization capability for model parameterization and monitoring system design.

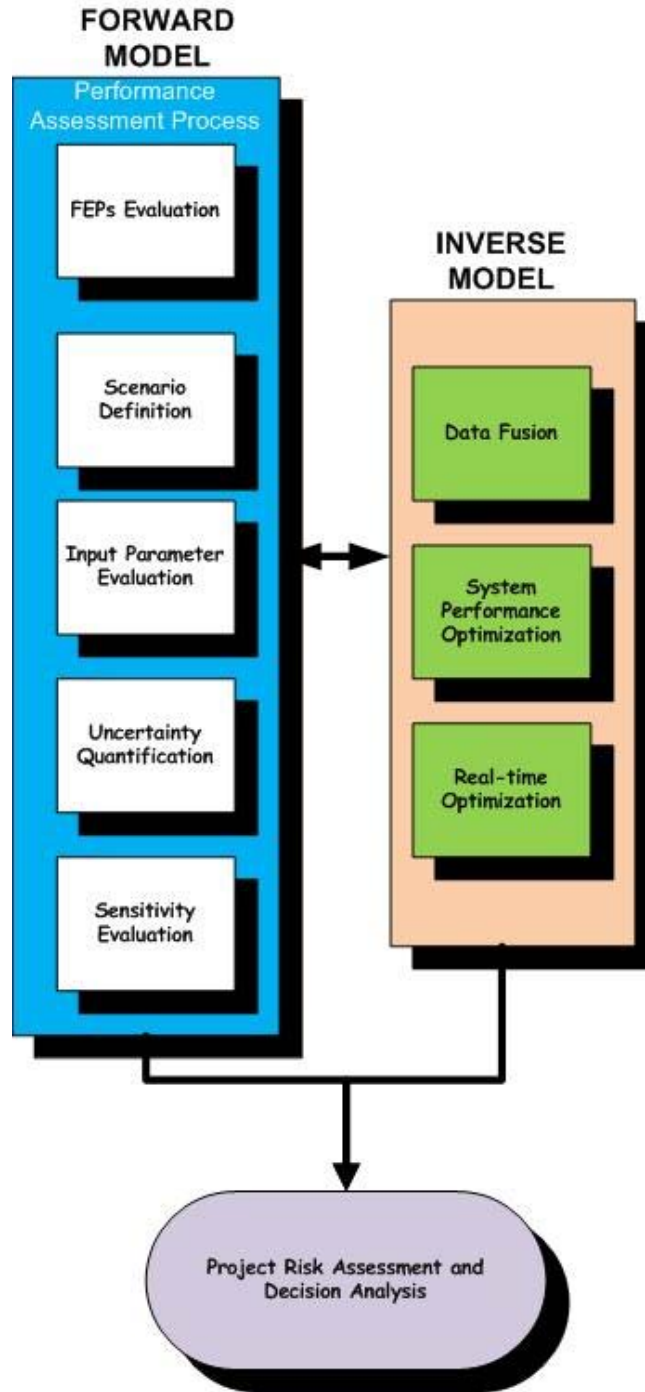


**Figure 2.** Enhanced Approach to Performance Assessment of Carbon Storage

The high-level architecture of the EPAS for carbon sequestration is shown in Figure 3. The system consists of three layers. The middle layer hosts detailed process models to capture all important physics involved in carbon sequestration. The bottom layer provides all necessary data to support process model runs. These two layers are then wrapped by a PA driver that is able to couple different process models, direct Monte-Carlo simulations, and assist PA analysis. As

discussed above, in order for the EPAS to be able to do inverse modeling, the PA driver must have a built-in optimization capability. For this reason, for the LDRD project described here, code DAKOTA version 4.0 was chosen to be the PA driver. DAKOTA (Design Analysis Kit for Optimization and Terascale Applications) is a powerful and versatile software toolkit that provides a flexible and extensible interface between simulation codes and iterative analysis methods used in large-scale systems engineering optimization, uncertainty quantification, and sensitivity analysis (Eldred et al, 2002). A full set of PA calculations impose stringent requirements on process code performance. The process codes must be robust and fast enough to run multiple model simulations in a widely spanned model parameter space. For the work documented here, TOUGH2 version 2.0 is used as the reservoir simulator.

The DAKOTA-TOUGH2 coupling allows for concurrent execution of code runs in a parallel computation mode when multiple CPUs are available. This scalable code execution mode allows fully coupled multiphase TOUGH2 simulations with various levels of complexity to be completed in a reasonable amount of time. Also, importantly, the TOUGH2 module ECO2N allows capturing the behavior of supercritical CO<sub>2</sub>.

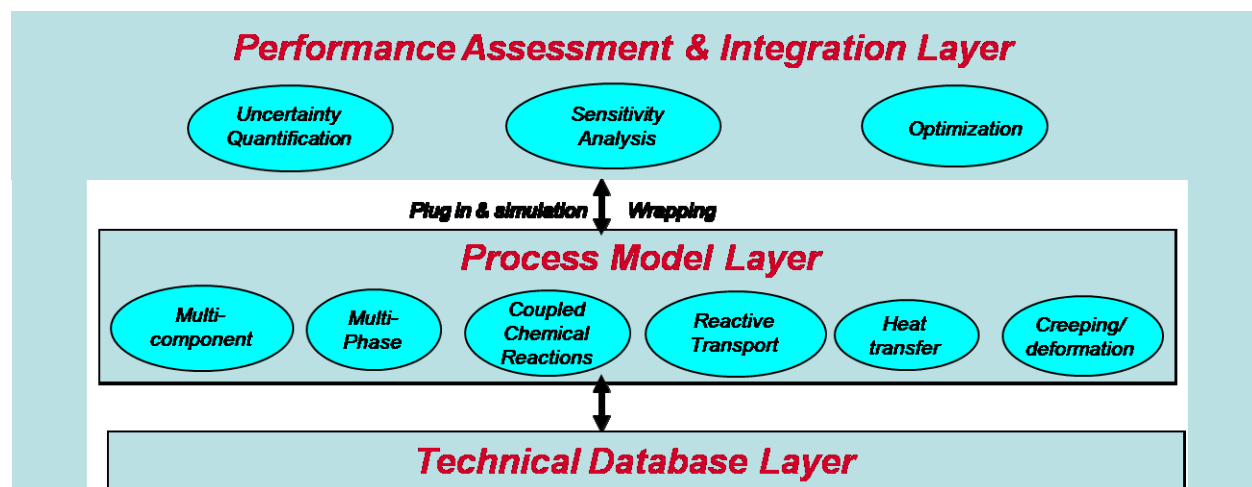


**Figure 3.** Enhanced Performance Assessment System (EPAS) Architecture

Following the general methodology illustrated in Figure 2, there are a number of steps to the research documented in this report. These steps include:

- Capture main features, events, and processes (FEPs) of a hypothetical carbon storage system by a systematic FEP analysis (see the FEP table in Section 3.2).
- Formulate major CO<sub>2</sub> injection, storage, and release scenarios (Section 3).
- Constrain parameter ranges and distributions of model input parameters (Sections 5.1 and 5.2).
- Run multiple simulations (Section 5).
  - Correlation between uncertainty parameters (e.g., permeability vs. porosity)
- Demonstrate uncertainty and sensitivity analyses (Section 5.4).
  - Performance parameters
  - 1

eters

- Reservoir pressure (t)
  - Leakage rate (t)
  - Quantity of CO<sub>2</sub> stored
  - Quantity of CO<sub>2</sub> leaked
- Identification of key input parameters
- Demonstrate optimization capability (planned as follow-on work) (Section 6).
  - Objective functions
    - Maximize total dissolved CO<sub>2</sub>.
    - Minimize the leakage.
    - Others

---

<sup>1</sup> Other important parameters such as cost of the system were not considered. Currently in the U.S., there is not a carbon tax or other mechanism in the U.S. to provide a metric for affordability of carbon sequestration projects. Projects could be evaluated based on the European carbon exchange (~13-15 Euros/ton (~\$16.50-\$19)) (European Climate Exchange, 2010), but that would not fully validate the projects for the U.S. market.



### 3. FEP ANALYSIS AND SCENARIO DEVELOPMENT

#### 3.1. Hypothetical Carbon Sequestration System

The potential storage system designs and conditions can be represented in a system architecture in many ways. Figure 4 shows one approach to discretizing the system for analysis purposes. From top to bottom in the figure, the overall system contains the engineered system consisting of an injection well, which is drilled into the geosphere. The system flow ultimately leads to the biosphere through a fault, abandoned unsealed well, or caprock. For simplification, fixed hydraulic pressures are imposed on the top surface of the shallow sandstone formation, while no flux condition is imposed on the bottom surface of the host rock. Fixed hydraulic pressures are imposed on both left and right sides, which are assumed to coincide with faults.

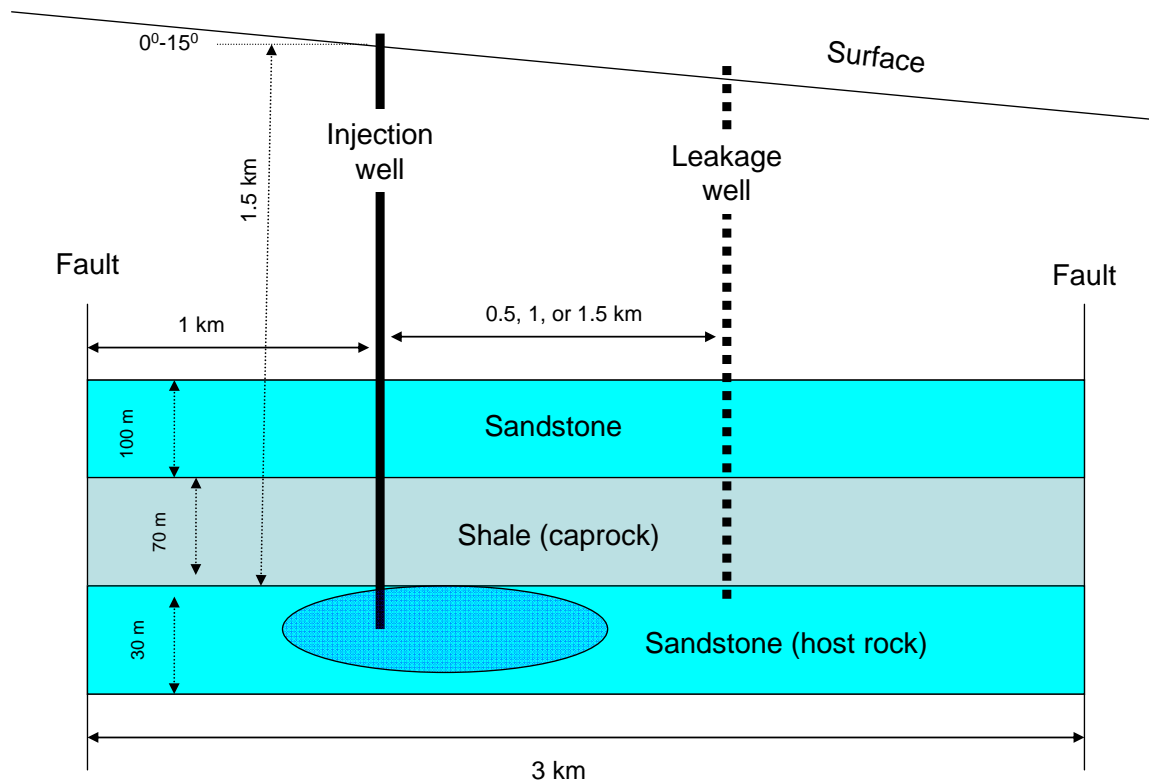


**Figure 4.** Schematic of Modeled System

The conceptual model of the generic CSS system is developed based on a site in eastern Texas, that is currently being investigated for suitability for carbon storage. The injection zone is into a brine-filled Oligocene Frio Formation (U.S. DOE, 2006). The site consists of a deep sandstone aquifer (targeted for  $\text{CO}_2$  storage), an overlying shale aquitard, and a shallow sandstone aquifer above the shale formation (see Figure 4).

### 3.2. Evaluation of FEPs

The features, events and processes (FEPs) that need to be included in this analysis were determined using the FEPs database developed by Quintessa (2010) as the basis. FEPs were either included or excluded based on the type of problem being considered. The full listing of FEPs included in this analysis is shown in Table 1 with a brief description of why the FEP was included.

**Table 1.** FEP Analysis

<b>FEP Class 0: Assessment Basis</b>		
<b>FEP Number</b>	<b>Description</b>	<b>Decision for Inclusion or Exclusion</b>
0.1	Purpose of the assessment	To provide a system-level assessment of the injectivity and the post-closure performance of a hypothetical CO <sub>2</sub> geological storage system.
0.2	Endpoints of interest	The capacity of the storage system and the magnitude and timing of fluxes of CO <sub>2</sub> escaping from the storage system.
0.3	Spatial domain of interest	Host rock and caprock (see Figure 4)
0.4	Timescale of interest	30 year injection, with 100 year total simulation time
0.5	Sequestration assumptions	Hydrologic trapping and dissolution; no mineral reactions and residual trapping
0.6	Future human action assumptions	Abandoned wells
0.7	Legal and regulatory framework	Not considered explicitly.
0.8	Model and data issues	A hypothetical carbon sequestration system based on the Frio site
<b>FEP Class 1.1: Geological Factors</b>		
<b>FEP Number</b>	<b>Description</b>	<b>Decision for Inclusion or Exclusion</b>
1.1.1	Neotectonics	Both left and right side boundaries coincide with growth faults
1.1.2	Volcanic and magmatic activity	Excluded Discrete seismic events are excluded from this analysis. However, the impact of overpressure on caprock integrity is included through an increased caprock permeability.
1.1.3	Seismicity	

1.1.4	Hydrothermal activity	Excluded
1.1.5	Hydrological and hydrogeological response to geological changes	Excluded
1.1.6	Large scale erosion	Excluded
1.1.7	Bolide impact	Excluded

**FEP Class 1.2: Climatic Factors**  
**FEP**

<b>Number</b>	<b>Description</b>	<b>Decision for Inclusion or Exclusion</b>
1.2.1	Global climate change	Excluded
1.2.2	Regional and local climate change	Excluded
1.2.3	Sea level change	Excluded
1.2.4	Periglacial effects	Excluded
1.2.5	Glacial and ice sheet effects	Excluded
1.2.6	Warm climate effects	Excluded
1.2.7	Hydrological and hydrogeological response to climate changes	Excluded
1.2.8	Responses to climate changes	Excluded

**FEP Class 1.3: Future Human Actions**  
**FEP**

<b>Number</b>	<b>Description</b>	<b>Decision for Inclusion or Exclusion</b>
1.3.1	Human influences on climate	Excluded
1.3.2	Motivation and knowledge issues	No societal memory of the storage assumed, and only inadvertent human intrusions are considered.
1.3.3	Social and institutional developments	Excluded
1.3.4	Technological developments	Excluded
1.3.5	Drilling activities	Assumed to be the most likely relevant human intrusion activity

1.3.6	Mining and other underground activities	Not explicitly considered. Impacts assumed to be covered by consideration of drilling activities (1.3.5).
1.3.7	Human activities in the surface environment	Excluded
1.3.8	Water management	Excluded
1.3.9	CO <sub>2</sub> presence influencing future operations	Excluded
1.3.10	Explosions and crashes	There are low probability events that are assumed to have possible consequences similar to seismic events.

**FEP Class 2.1: CO<sub>2</sub> Storage Pre-Closure FEP**

<b>Number</b>	<b>Description</b>	<b>Decision for Inclusion or Exclusion</b>
2.1.1	Storage Concept	The model is applicable to a range of different storage systems.
2.1.2	CO <sub>2</sub> quantities, injection rate	The total amount of CO <sub>2</sub> injected is a model input.
2.1.3	CO <sub>2</sub> composition	Pure CO <sub>2</sub> assumed.
2.1.4	Microbiological contamination	Excluded
2.1.5	Schedule and planning	Not explicitly considered
2.1.6	Pre-closure administrative control	Not explicitly considered
2.1.7	Pre-closure monitoring of storage	Any monitoring wells will be considered as an abandoned well.
2.1.8	Quality control	Not explicitly considered
2.1.9	Accidents and unplanned events	Excluded
2.1.10	Over-pressuring	Over-pressures due to the amounts of CO <sub>2</sub> injected will be calculated by the model.

**FEP Class 2.2: CO<sub>2</sub> Storage Post Closure FEP**

<b>Number</b>	<b>Description</b>	<b>Decision for Inclusion or Exclusion</b>
2.2.1	Post-closure administrative control	No administrative controls are assumed post-closure.
2.2.2	Post-closure monitoring of storage	No post-closure monitoring is assumed.

2.2.3	Records and markers	No records and markers are assumed
2.2.4	Reversibility	Outside the assessment context.
2.2.5	Remedial actions	Outside the assessment context.

**FEP Class 3.1: CO<sub>2</sub> Properties**  
**FEP**

<b>Number</b>	<b>Description</b>	<b>Decision for Inclusion or Exclusion</b>
3.1.1	Physical properties of CO <sub>2</sub>	The variation of CO <sub>2</sub> viscosity is calculated as a function of pressure and temperature.
3.1.2	CO <sub>2</sub> phase behaviour	The variation of CO <sub>2</sub> density is calculated as a function of pressure and temperature.
3.1.3	CO <sub>2</sub> solubility and aqueous speciation	Dissolution in water is represented explicitly. Dissolution in oil is not considered.

**FEP Class 3.2: CO<sub>2</sub> Interactions**  
**FEP**

<b>Number</b>	<b>Description</b>	<b>Decision for Inclusion or Exclusion</b>
3.2.1	Effects of pressurization of reservoir on caprock	Implicitly included. The effects will be incorporated as an increase in caprock permeability.
3.2.2	Effects of pressurization on reservoir fluids	Induced groundwater flows will be calculated.
3.2.3	Interaction with hydrocarbons	Outside the assessment context.
3.2.4	Displacement of saline formation fluids	Included. The volume of brine displaced is a performance parameter.
3.2.5	Mechanical processes and conditions	Part of it is implicitly included as damage to caprock.
3.2.6	Induced seismicity	Excluded
3.2.7	Subsidence or uplift	Excluded
3.2.8	Thermal effects on injection point	Temperature is calculated based on geothermal gradient.
3.2.9	Water chemistry	Included in CO <sub>2</sub> solubility calculations
3.2.10	Interaction of CO <sub>2</sub> with chemical barriers	Salt precipitation due to dryout is included.
3.2.11	Sorption and desorption of CO <sub>2</sub>	Excluded Not explicitly included. It can be estimated from the calculated CO <sub>2</sub> pressure and the amount of CO <sub>2</sub> dissolved outside the PA calculations.
3.2.12	Heavy metal release	

3.2.13	Mineral phase	Mineral trapping of CO <sub>2</sub> is ignored.
3.2.14	Gas chemistry	Will affect CO <sub>2</sub> solubility and thus included implicitly in some process algorithms.
3.2.15	Gas stripping	Outside the assessment context.
3.2.16	Gas hydrates	Any formation of gas hydrates is assumed to be unimportant on the timescales of interest.
3.2.17	Biogeochemistry	Not represented explicitly.
3.2.18	Microbial processes	Not represented explicitly. Methanogenesis is conservatively assumed not to occur (thereby maximizing the amount of stored CO <sub>2</sub> ).
3.2.19	Biomass uptake of CO <sub>2</sub>	Excluded

**FEP Class 3.3: CO<sub>2</sub> Transport**  
**FEP**

<b>Number</b>	<b>Description</b>	<b>Decision for Inclusion or Exclusion</b>
3.3.1	Advection of free CO <sub>2</sub>	Not explicitly included due to the limitation of TOUGH2
3.3.2	Buoyancy-driven flow	Vertical transport of free CO <sub>2</sub> due to buoyancy forces is directly represented.
3.3.3	Displacement of formation fluids	Included
3.3.4	Dissolution in formation fluids	Dissolution of CO <sub>2</sub> in groundwater is represented explicitly.
3.3.5	Water mediated transport	Advection of dissolved CO <sub>2</sub> in groundwater is represented explicitly.
3.3.6	CO <sub>2</sub> release processes	Included.
3.3.7	Co-migration of other gases	Excluded

**FEP Class 4.1: Geology**  
**FEP**

<b>Number</b>	<b>Description</b>	<b>Decision for Inclusion or Exclusion</b>
4.1.1	Geographical location	The model can be applied to any location.
4.1.2	Natural resources	Included in defining human intrusion scenarios and probabilities.
4.1.3	Reservoir type	Represented explicitly.
4.1.4	Reservoir geometry	Represented explicitly.

4.1.5	Reservoir exploitation	Represented implicitly in the human intrusion scenario.
4.1.6	Cap rock or sealing formation	Represented explicitly.
4.1.7	Additional seals	Represented explicitly.
4.1.8	Lithology	Properties of all rocks in the system domain are represented explicitly or implicitly.
4.1.9	Unconformities	Represented implicitly in rock properties.
4.1.10	Heterogeneities	Represented by varying properties of model compartments.
4.1.11	Faults and fractures	Represented implicitly in rock permeability and boundary conditions
4.1.12	Undetected features	The importance of undetected features can be assessed by varying the representation of the system geology.
4.1.13	Vertical geothermal gradient	Represented explicitly.
4.1.14	Formation pressure	Represented explicitly.
4.1.15	Stress and mechanical properties	Included implicitly in some process algorithms.
4.1.16	Petrophysical properties	Represented explicitly.

**FEP Class 4.2: Fluids**

**FEP**

<b>Number</b>	<b>Description</b>	<b>Decision for Inclusion or Exclusion</b>
4.2.1	Fluid properties	Represented explicitly.
4.2.2	Hydrogeology	Represented explicitly
4.2.3	Hydrocarbons	Outside assessment context.

**FEP Class 5.1: Drilling and Completion**

**FEP**

<b>Number</b>	<b>Description</b>	<b>Decision for Inclusion or Exclusion</b>
5.1.1	Formation damage	Included in the initial conditions if relevant.
5.1.2	Well lining and completion	Not represented explicitly, but included implicitly in borehole permeability
5.1.3	Workover	Any effects relevant to the initial conditions will be included implicitly.

5.1.4	Monitoring wells	May need to be represented in the system description.
5.1.5	Well records	Screened out. No memory of the sequestration is assumed.

**FEP Class 5.2: Borehole Seals and Abandonment**  
**FEP**

<b>Number</b>	<b>Description</b>	<b>Decision for Inclusion or Exclusion</b>
5.2.1	Closure and sealing of boreholes	Not represented explicitly, but included implicitly in borehole failure rate
5.2.2	Seal failure	Included in borehole failure rate and permeability changes.
5.2.3	Blowouts	Not explicitly considered
5.2.4	Orphan wells	Included as abandoned boreholes
5.2.5	Soil creep around boreholes	Not considered

**FEP Class 6.1: Terrestrial Environment**  
**FEP**

<b>Number</b>	<b>Description</b>	<b>Decision for Inclusion or Exclusion</b>
6.1.1	Topography and morphology	Represented in a simplified way.
6.1.2	Soils and sediment	Excluded.
6.1.3	Erosion and deposition	Excluded
6.1.4	Atmosphere and meteorology	Excluded
6.1.5	Hydrological regime and water balance	Implicitly represented by groundwater flow
6.1.6	Near-surface aquifers and surface water bodies	Not explicitly represented
6.1.7	Terrestrial flora and fauna	Not considered
6.1.8		

**FEP Class 6.2: Marine Environment**  
**FEP**

<b>Number</b>	<b>Description</b>	<b>Decision for Inclusion or Exclusion</b>
---------------	--------------------	--



6.2.1	Coastal features	Excluded
6.2.2	Local oceanography	Excluded
6.2.3	Marine sediments	Excluded
6.2.4	Marine flora and fauna	Excluded
6.2.5	Marine ecological systems	Excluded

**FEP Class 6.3: Human Behaviour**

**FEP**

<b>Number</b>	<b>Description</b>	<b>Decision for Inclusion or Exclusion</b>
6.3.1	Human characteristics	Calculations do not consider impacts on humans, therefore no description of human behavior is required.
6.3.2	Diet and food processing	Calculations do not consider human behavior.
6.3.3	Lifestyles	Calculations do not consider human behavior.
6.3.4	Land and water use	Calculations do not consider human behavior.
6.3.5	Community characteristics	Calculations do not consider human behavior.
6.3.6	Buildings	Calculations do not consider human behavior.

**FEP Class 7.1: System Performance**

**FEP**

<b>Number</b>	<b>Description</b>	<b>Decision for Inclusion or Exclusion</b>
7.1.1	Loss of containment	Represented explicitly.

**FEP Class 7.2: Impacts on the Physical Environment**

**FEP**

<b>Number</b>	<b>Description</b>	<b>Decision for Inclusion or Exclusion</b>
7.2.1	Contamination of groundwater	Only for dissolved CO <sub>2</sub> .
7.2.2	Impacts on soils and sediments	Outside assessment context.
7.2.3	Release to the atmosphere	The model calculates the total CO <sub>2</sub> release from the storage.

7.2.4	Impacts on exploitation of natural resources	Excluded
7.2.5	Modified hydrology and hydrogeology	Represented explicitly.
7.2.6	Modified geochemistry	Implicitly included.
7.2.7	Modified seismicity	Excluded
7.2.8	Modified surface topography	Excluded

**FEP Class 7.3: Impacts on Flora and Fauna**  
**FEP**

<b>FEP Number</b>	<b>Description</b>	<b>Decision for Inclusion or Exclusion</b>
7.3.1	Asphyxiation effects	Impacts on flora and fauna not calculated.
7.3.2	Effect of CO <sub>2</sub> on plants and algae	Impacts on flora and fauna not calculated.
7.3.3	Ecotoxicology of contaminants	Impacts on flora and fauna not calculated.
7.3.4	Ecological effects	Impacts on flora and fauna not calculated.
7.3.5	Modification of microbiological systems	Impacts on flora and fauna not calculated.

**FEP Class 7.3: Impacts on Humans**  
**FEP**

<b>FEP Number</b>	<b>Description</b>	<b>Decision for Inclusion or Exclusion</b>
7.3.1	Health effects of CO <sub>2</sub>	Impacts on humans not calculated.
7.3.2	Toxicity of contaminants	Impacts on humans not calculated.
7.3.3	Impacts from physical disruption	Impacts on humans not calculated.
7.3.4	Impacts from ecological modification	Impacts on humans not calculated.

### 3.3. Scenario Description

The basic scenario for this analysis includes a caprock overlying the potential injection zone, and a vertical fault on the boundary of the injection zone. The scenario also includes the potential for CO<sub>2</sub> release from an abandoned borehole in the formation. The location of the abandoned well

can be considered uncertain. However, for this evaluation a value of 1km distance from the injection well was used. A time period of 30 years duration for injection, and a total simulation time of 100 years was evaluated.

Other scenarios to be evaluated in future work include analysis of additional abandoned wells, additional injection wells and alternative injection rates, potential for leakage from the caprock due to overpressuring or lack of caprock integrity, inclusion of heterogeneities in the injection zone, and alternative cost models for the injection/monitoring facilities. The base case as well as some of these additional scenarios are listed in Table 2.

**Table 2.** Sequestration Scenarios

<b>Number</b>	<b>Scenarios</b>	<b>Description</b>
1	Base case	Injection to base case system, with potential for release along distant fault system or a single abandoned well.
2	Multiple abandoned, leaking boreholes	Injection to base case system with potential for release from multiple abandoned, degraded closed wells.
3	Leaking caprock	Overpressure the system due to injection rates, and allow leakage through the caprock.
4	Impact on upper groundwater aquifer	Injection through the system escapes to hypothetical upper groundwater aquifer, and impacts the water chemistry in the aquifer.
5	Heterogeneous injection zone	Modify the injection zone to include heterogeneities in permeability/porosity.
6	Surface facility optimization	Incorporate surface facilities, including cost and alternative injection rates.

## 4. DEVELOPMENT OF PROTOTYPE EPAS

The prototype of EPAS was developed by wrapping an existing multi-phase, multi-component reservoir simulator (TOUGH2) with an uncertainty quantification and optimization code (DAKOTA).

### 4.1. Description of TOUGH2

TOUGH2 is a widely used numerical simulator for a variety of problems (Pruess et al, 1999). The simulator facilitates modeling of nonisothermal flows of multicomponent, multiphase fluids in one, two, and three dimensional porous and fractured media. The simulator includes several equation-of-state (EOS) modules, including one that allows injection of CO<sub>2</sub> and simulation of all the surrounding processes. This EOS specific to CO<sub>2</sub> is the so-called ECO2N module (Pruess, 2005), and is a fluid property module designed for applications of geologic sequestration of CO<sub>2</sub> in saline aquifers. For this analysis, TOUGH2 version 2.0 was utilized.

### 4.2. Description of DAKOTA

DAKOTA (Design Analysis Kit for Optimization and Terascale Applications) is a software toolkit that provides a flexible and extensible interface between simulation codes and iterative analysis methods used in large-scale systems engineering optimization, uncertainty quantification, and sensitivity analysis (Eldred et al, 2002). The DAKOTA toolkit can perform parameter optimization through the use of gradient and nongradient-based methods. It can also be used to conduct sensitivity analysis with the purpose of investigating variability in response to variations in model parameters using sampling methods such as Latin Hypercube Sampling (LHS), among others. Further capabilities of the toolkit include uncertainty quantification with sampling, analytic reliability, and stochastic finite element methods; and parameter estimation with nonlinear least squares methods. These capabilities may be used on their own or as components within system models. By employing object oriented design to implement abstractions of the key components required for iterative systems analyses, the DAKOTA toolkit provides a flexible and extensible problem-solving environment for design and performance analysis of computational models on high performance computers. For this analysis, DAKOTA version 4.0 was utilized.

### 4.3. Wrapping TOUGH2 with DAKOTA

Specific to this study, a DAKOTA based nondeterministic sampling algorithm is implemented for the enhanced performance assessment (EPAS) framework. Figure 5 schematically depicts the overall scheme of how DAKOTA is coupled to TOUGH2. The overall sampling flow involves embedded TOUGH2 functional evaluations within a DAKOTA run. First, a set of uncertain parameters with assigned probability distributions is specified in the DAKOTA input parameter file. A sample is drawn using Latin Hypercube sampling (LHS). The sample is processed by an input filter routine to transcribe each sample element, comprising a value for each uncertain parameter, into a formatted template file that is compatible with TOUGH2. After each sample element is executed, an output filter extracts the pertinent output values via an output filter routine and returns these to DAKOTA.

LHS can be described as a stratified sampling method where the range of each variable to be sampled is divided into intervals of equal probability and a value is randomly sampled from each interval (Adams et al., 2010). Sampled values are randomly paired for different variables to form sample elements. Overall, LHS needs fewer samples relative to other random sampling methods (e.g., Monte Carlo) to obtain statistically stable estimates of mean values and has become widely used in uncertainty analysis. DAKOTA summarizes the statistical spread of the output observations at the completion of each DAKOTA run.

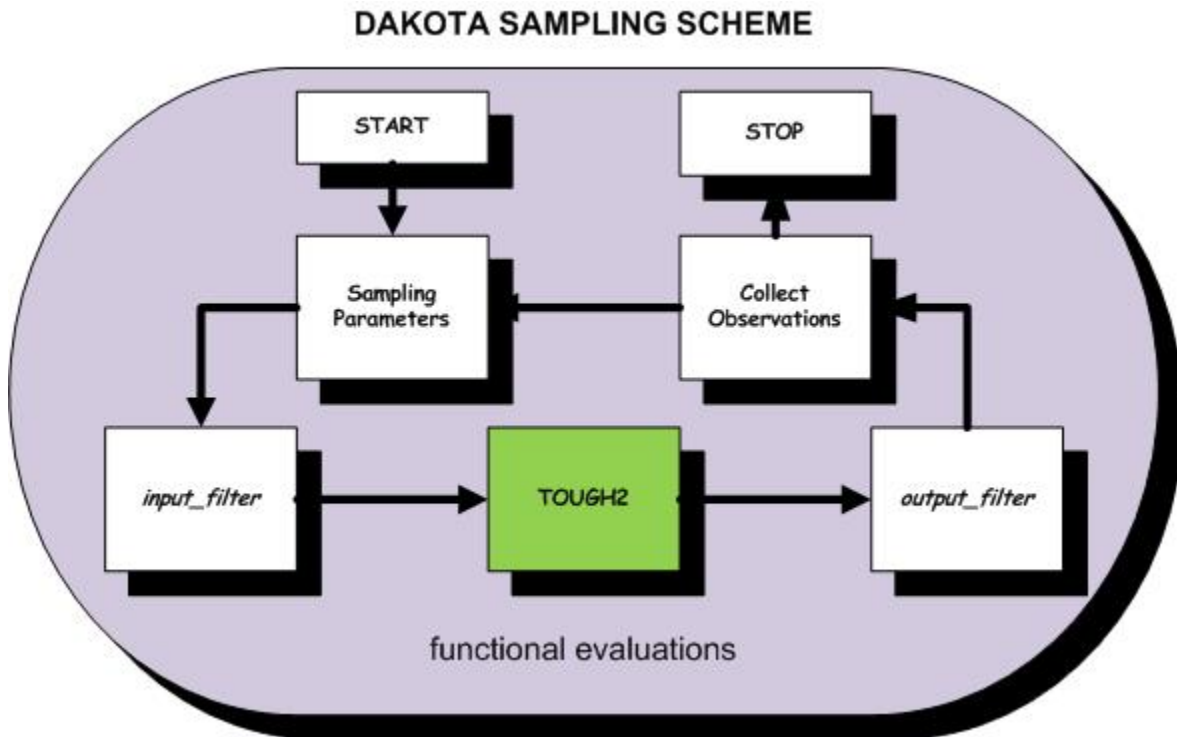


**Figure 5.** Schematic of DAKOTA-based EPAS framework

#### **4.4. Parallel Version of DAKOTA-TOUGH2**

DAKOTA is designed to support large-scale simulations that can be computationally intensive. Different levels of parallelism are available for users to utilize in DAKOTA. For the EPAS framework, a hybrid parallelism is assumed. Figure 6 shows how the flow of information works in a hybrid implementation. Extraction scripts embedded in the DAKOTA simulation script were also developed for the extraction of TOUGH2 outputs in each code run.

## DAKOTA – TOUGH2 HYBRID PARALLELISM

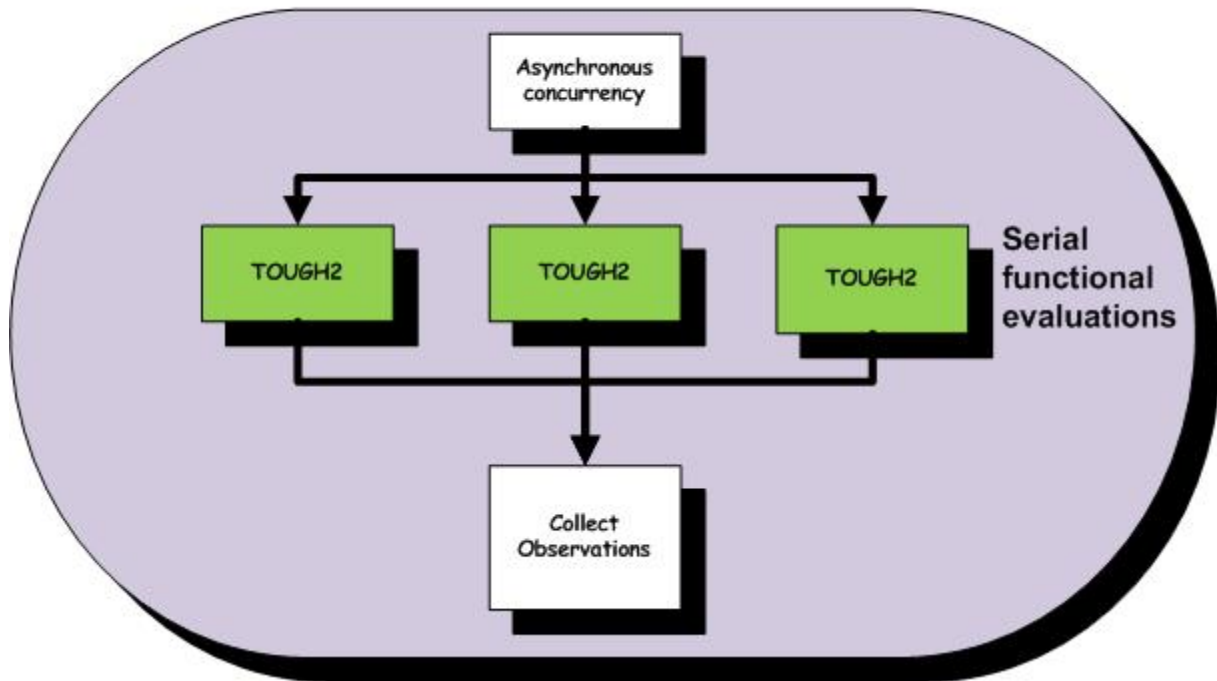


**Figure 6.** Schematic of hybrid parallelism used in the CSS-PA study

Specification of asynchronous concurrency within DAKOTA provides a level of parallelism at functional evaluation level. Three concurrent serial TOUGH2 (T2) jobs can be executed at any given time as long as the computational CPUs are available. This level of parallelism essentially shortens the overall calculation cycle. Such coupling can further be refined and expanded to run in parallel on the high-performance computational clusters at SNL.

## 5. DEMONSTRATION OF PROTOTYPE EPAS

### 5.1. General Description of the Model

Here we present a hypothetical conceptual and numerical model of the carbon sequestration system that we used to demonstrate feasibility for our coupled reservoir-optimization portion of the PA model. This conceptual model is a simplified version of a proposed benchmark problem for CO<sub>2</sub> injection and storage discussed by Class et al. (2009) and is used to develop input for a numerical model, as well to help guide evaluation of uncertainty of a variety of relevant parameters as identified in Table 3. This is designed to be generally applicable to subsurface carbon storage pilot projects currently underway as part of DOE/NETL's partnerships for carbon sequestration (NETL, 2010a). Petrophysical parameters and spatial heterogeneity were chosen to loosely correspond to the Frio pilot injection project near the Texas Gulf Coast, USA involving the Oligocene Frio Formation as storage reservoir and the overlying Miocene Anahuac Formation as caprock. Parameter values are listed in Table 3.

**Table 3.** List of Input Parameters

Input parameter	Value	Note
Physical configuration & geologic setting		
Length	3 km	
Dip	0	No dip
Thickness of host rock	30 m	
Thickness of caprock	70 m	
Thickness of shallow aquifer	100 m	
Depth at top of host rock at injection well	1.5 km	
Distance of leakage well from injection well	1.0 km	A fixed location selected
Temperature	25 °C	A constant temperature selected
Salinity of brine	20,000 ppm	A constant value selected for the host rock only
Velocity of brine flow	0	No regional ground water flow considered
Operational conditions		
Injection rate	0.05 – 0.3 kg/s	Uniform dist.
Productivity index	$1 \times 10^{-12} - 2 \times 10^{-12} \text{ m}^3$	Uniform dist.
Flowing wellbore pressure	≈15 MPa	Constant – hydrostatic for each element
Duration of brine-CO <sub>2</sub> injection cycle	30 years	Injection followed by 70 years of observation

Injection depth	1512 m-1522 m	Below surface
Hydrologic properties		
Reservoir Average Porosity	0.322	Constant
Reservoir Average horizontal permeability	$3.12 \times 10^{-13} \text{ m}^2$	Constant
Reservoir Average vertical permeability	$3.12 \times 10^{-13} \text{ m}^2$	Constant
Reservoir Residual water saturation	0.0	Constant
Reservoir Residual gas saturation	0.222	Constant
Reservoir van Genuchten parameter $\lambda$	0.43	Constant
Reservoir van Genuchten parameter $1/P_0$	$1.45 \times 10^{-5} \text{ Pa}^{-1}$	Constant
Caprock porosity	Range: 0.01-0.10; mean: 0.055; std dev: 0.0225	Normal dist.
Caprock permeability	Range: $5 \times 10^{-16} - 5 \times 10^{-15} \text{ m}^2$ ; mean: $1.1802 \times 10^{-15} \text{ m}^2$ ; std dev: $6.807 \times 10^{-16} \text{ m}^2$	Lognormal dist.
Caprock Residual water saturation	0.0 - 0.3	Uniform dist.
Caprock Residual gas saturation	0.2	Constant
Caprock van Genuchten parameter $\lambda$	0.40	Constant
Caprock van Genuchten parameter $1/P_0$	$1.61 \times 10^{-5} \text{ Pa}^{-1}$	Constant
Aquifer Average Porosity	0.322	Constant
Aquifer Average permeability	$3.12 \times 10^{-13} \text{ m}^2$	Constant
Aquifer Residual water saturation	0.0	Constant
Aquifer Residual gas saturation	0.222	Constant
Aquifer van Genuchten parameter $m$	0.43	Constant
Aquifer van Genuchten parameter $1/P_0$	$1.45 \times 10^{-5} \text{ Pa}^{-1}$	Constant
Fluid properties		
Critical pressure of CO <sub>2</sub>	7.38 MPa	
Critical pressure of brine	22.09 MPa	
Critical temperature of CO <sub>2</sub>	31.05 °C	
Critical temperature of brine	374.2 °C	
Critical volume of CO <sub>2</sub>	$9.4 \times 10^{-5} \text{ m}^3/\text{mol}$	



Critical volume of brine	$5.6 \times 10^{-5} \text{ m}^3/\text{mol}$	
Other parameters		
Time scale for model simulation	100 years	

## 5.2. General Attributes of the Model

### *Computational Model and Ranges of Parameters*

To demonstrate feasibility of the approach, we constructed a 2D model based on the commonly used storage reservoir – caprock- overlying aquifer conceptual model. For our purposes, our simulation domain is a 3000 m by 200 m rectangular domain 1330 m below ground surface (Figure 7; also Figure 4). The reservoir is taken to be 30 m thick, with both homogeneous and heterogeneous properties. The overlying caprock, with homogeneous properties, is 70 m thick, and the aquifer, at the top of the domain, is taken to be 100 m thick. A finite volume grid used in the numerical simulations discussed below is shown superimposed upon the three spatial regions. Injection of supercritical CO<sub>2</sub> (scCO<sub>2</sub>), a leaky well scenario, cap rock leakage, and brine and CO<sub>2</sub> migration driven by injection- related rise in pressure are three aspects of the conceptual model that are investigated by numerical means. The 2D nature of the simulation domain could represent a slice impacted by injection from a horizontal well oriented in the out-of-plane direction.

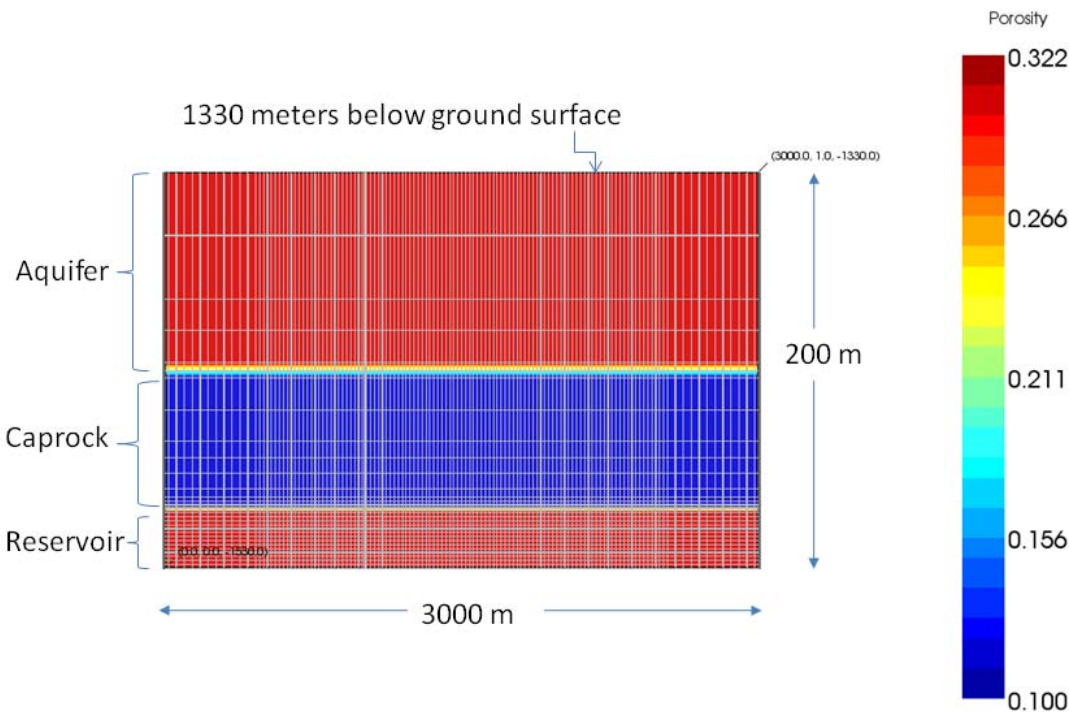


**Figure 7.** Conceptual reservoir-caprock-aquifer model for subsurface carbon storage, with superimposed numerical grid for TOUGH2 simulations.

Ranges in porosity, permeability, capillary pressure-saturation curves, and relative permeability that will be used in the numerical modeling are taken from values determined by the Texas Bureau of Economic Geology as presented by Holtz et al. (2005). Mean values for the storage reservoir correspond to those from the upper portion of the Frio Formation, while the lowest value for the caprock is taken to be that for the overlying Anahuac Formation. Higher values of caprock permeability would result from, e.g., natural or induced fractures, an important leakage scenario. Values for the “aquifer” region are taken to equal the mean porosity from the upper Frio as given by Holtz et al. (2005). These are summarized in Table 4.

**Table 4.** Petrophysical parameters for the upper Frio Formation and Anahuac Formation shale (after Holtz et al., 2005)

Parameter	Clean Upper Frio	“Shaley” Frio	Anahuac Formation
Mean Porosity	0.322		0.100
Mean Permeability, m <sup>2</sup>	3.12x10 <sup>-13</sup>	1.67x10 <sup>-14</sup>	5.29x10 <sup>-16</sup>
S <sub>is</sub> <sup>1</sup>	0.999	0.999	0.999
P <sub>o</sub> (psi) <sup>1</sup>	10	10	4000
λ <sup>1</sup>	0.43	0.43	0.67
S <sub>ir</sub> (residual water saturation) <sup>1</sup>	0.08	0.54	0.0
S <sub>gr</sub> (residual gas saturation) <sup>1</sup>	0.20	0.20	0.10

<sup>1</sup>S<sub>is</sub>, P<sub>o</sub>, λ, S<sub>ir</sub>, and S<sub>gr</sub> are parameters in the Van Genuchten (1980) model for capillary pressure and relative permeability.

### *Multiphase Flow Parameters*

For multiphase flow parameters (capillary pressure curves, and relative permeability), we apply the van Genuchten formulation (van Genuchten, 1980) to the experimental results given by Holtz et al. (2005). Although we did not attempt rigorous curve fits to extract parameters, the parameters given in Table 4 were found by a quick trial and error visual fit to several data points from capillary pressure curves; these are shown in Figure 8. Interestingly, the curves for the “Clean” and “Shaly” Frio of Holtz et al. (2005) can both be fit just by modifying the residual water saturation. These parameters are summarized in Table 4.

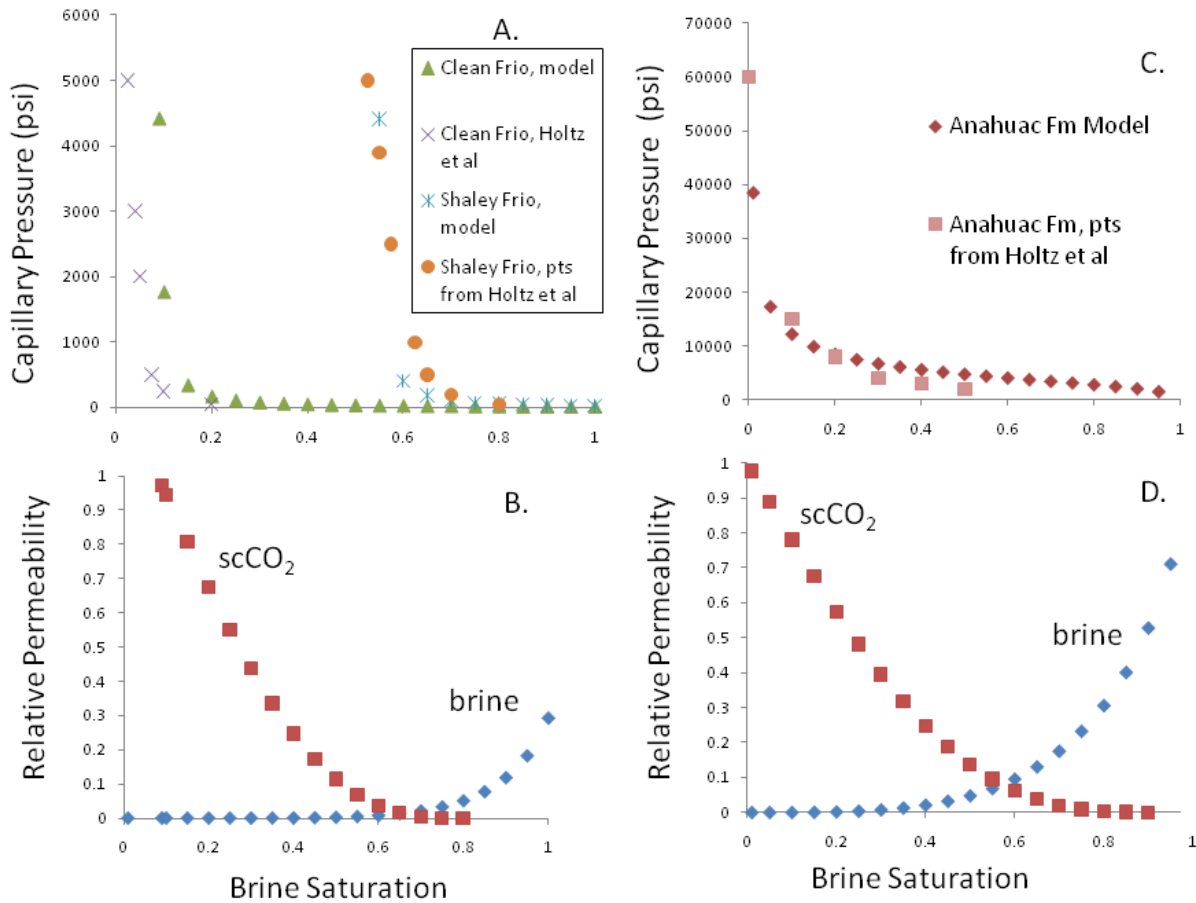


**Figure 8.** A. Capillary pressure curves for “Clean” and “Shaly” Frio Formation sands showing select data points from Holtz et al. (2005) and corresponding fit to van Genuchten formation. B. Corresponding gas and liquid relative permeability for the upper Frio “Clean” sand plotted as a function of liquid, or brine, saturation. C. Capillary pressure function for Anahuac Formation shale, via select data points, and corresponding fit to van Genuchten formulation. D. Gas and liquid relative permeability for Anahuac Formation as determined using capillary pressure curve parameters.

### *Heterogeneity in Reservoir Properties*

Because subsurface carbon storage involves a certain degree of uncertainty in storage reservoir properties (as most saline formations are not targets of exploration for resources like petroleum and water), we need to account for heterogeneity in reservoir properties like porosity, permeability, and capillary pressure. Distributions of porosity and permeability, and their cross-correlation for the Frio example, are taken from well log and core plug measurements as given by Holtz et al. (2005). Such data are generally analyzed for their spatial correlation using autocorrelation functions or so-called variograms which describe graphically how porosity and permeability vary spatially. One method to include heterogeneity in petrophysical properties for flow simulations is to use a variogram for a particular sedimentary facies, along with distributions of porosity and permeability and their correlation, to generate multiple realizations of porosity and permeability fields. This is beyond the scope of the current work; for our purposes here we have generated one such realization using the geostatistical technique

“Sequential Gaussian Simulation” via the SGSIM program, part of the GSLIB software package (Deutsch and Journel, 1998). A correlated permeability is obtained using the coregionalization method that uses a relationship between core and wireline log porosity values and permeability measurements made on core, producing spatially correlated permeability values (Rautman and McKenna, 1997). This was done with the COREG5 software provided by Sean McKenna of Sandia National Laboratories (McKenna, 2010). Capillary pressure heterogeneity can be derived from the porosity and permeability fields using the Leverett “J” function as is commonly used in petroleum engineering (Saadatpour et al., 2007). Although not described in detail here, we have found that the Leverett “J” method can be reconciled with the experimental capillary pressure data of Holtz et al. (2005) by varying only the residual water saturation.

### Numerical Solution

For numerical solution of the partial differential equations describing injection of supercritical CO<sub>2</sub> (scCO<sub>2</sub>), immiscible displacement of subsurface brines, and subsequent fate and transport of scCO<sub>2</sub> in our simple model, we use the finite volume method and TOUGH2 reservoir simulator (Pruess et al., 1999) along with the ECO2N equation of state module (Pruess, 2005). We employ a 2D grid with 4160 cells (shown in Figure 7) which is fairly coarse, but permits numerical convergence over a range of parameters, that we can use to demonstrate feasibility of our approach. Heterogeneity in porosity and permeability are mapped onto the TOUGH2 grid using the GSLIB software described previously by discretizing the distributions in terms of 20 distinct material types. Frequency distributions of values of porosity and permeability determined by this method are shown in Figure 9.

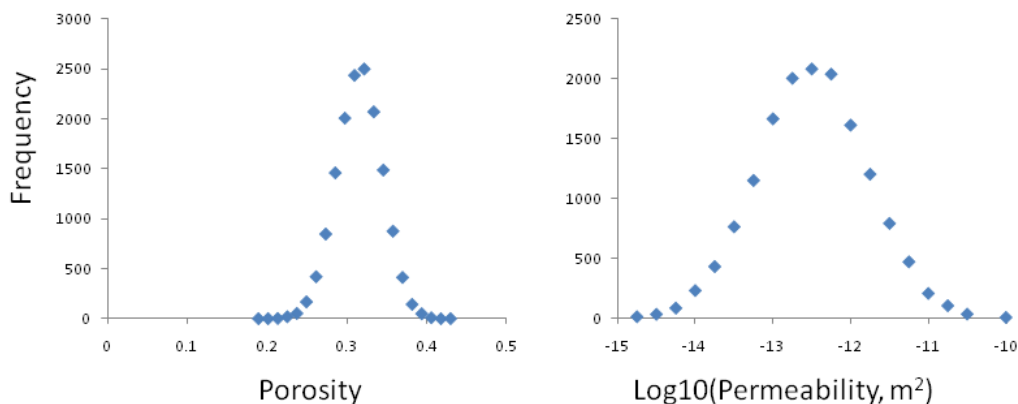


**Figure 9.** Frequency distributions of porosity and permeability used in 20 TOUGH2 material properties.

Injection is accomplished by means of 5 cells with a constant injection rate, and a leaky well scenario is investigated using the “well-on-delivery” capability of TOUGH2. We employ a leakage rate that is proportional to the fluid pressure above hydrostatic and a productivity index that is a function of the permeability of the cells surrounding the leaky well cells. For our purposes here, leakage is only to the surface, and not through the caprock into the overlying aquifer. Also included are so-called FOFT cells, used to obtain time dependent cell-specific output during a TOUGH2 run. These, along with plots showing an example of spatial

heterogeneity in porosity and permeability in the simulated upper Frio reservoir, are shown in Figure 10, and are used in an example simulation in the next section.

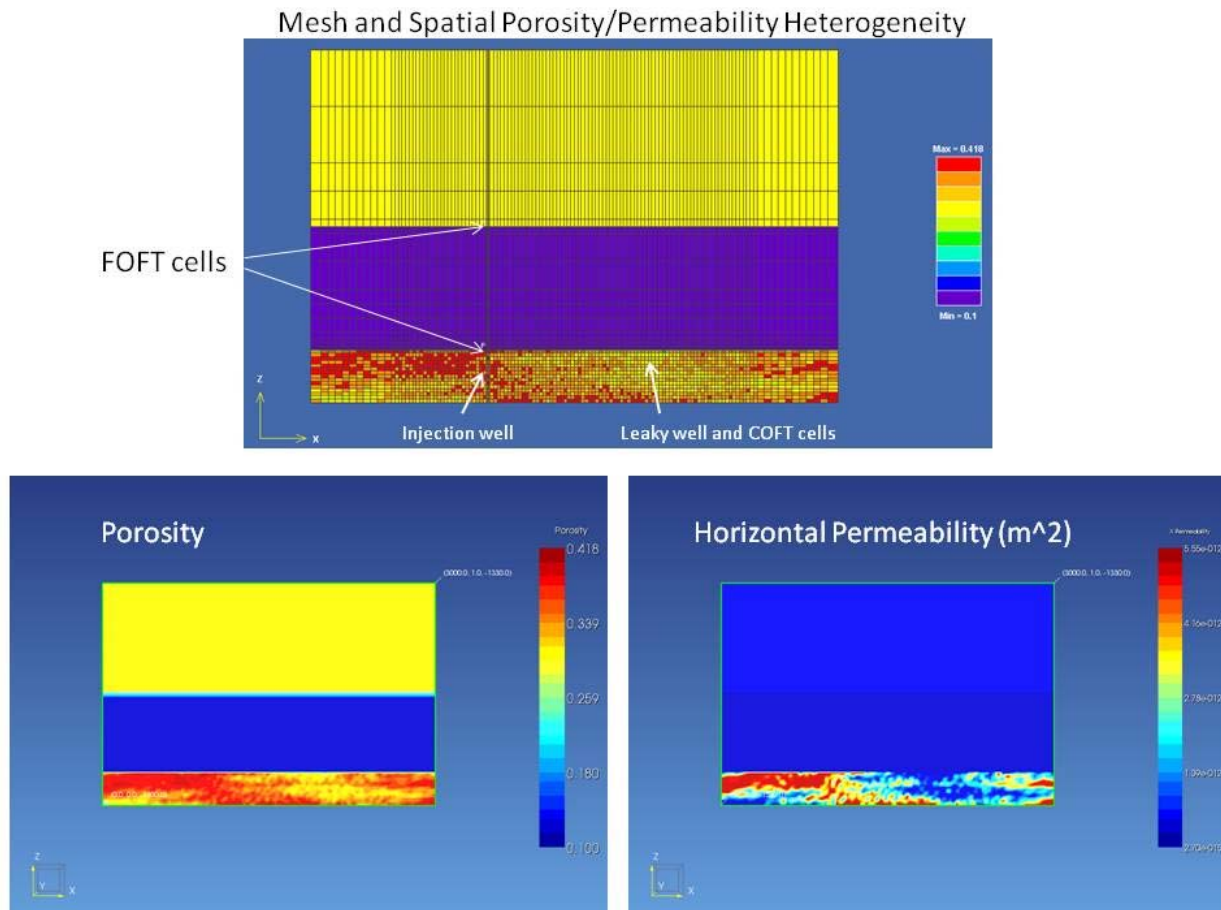


**Figure 10.** Mesh, location of injection and leaky wells, FOFT cells, and spatial heterogeneity in porosity and permeability in the storage reservoir.

### 5.3. Results of EPAS demonstration

#### 5.3.1. Deterministic case

An example of CO<sub>2</sub> injection using the 2D model in Figure 10 is shown in the next two figures. The injection rate for this example was 0.35 kg/s and was distributed equally over 5 cells. Permeability of the caprock was fairly high in this example, equal to  $2.7 \times 10^{-15} \text{ m}^2$ . The van Genuchten  $\lambda$  parameter was taken to be equal to 0.67, as given in Table 4 for the Anahuac Formation. A fairly substantial overpressure, equal to 21 MPa, develops adjacent to the injection well (Figure 11A). This exceeds the hydrostatic pressure beneath the caprock ( $\sim 15 \text{ MPa}$ ) by a significant amount and, depending on the horizontal stress regime, may be getting close to a level large enough to induce fracturing near the wellbore. This dissipates after about 10 years largely due to leakage through the caprock so that pressures return to near hydrostatic. The

influence of the leaky well is evident in the asymmetric pressure; the productivity index chosen for this run is high enough so that well release buffers the zone downstream from any injection-related pressure increase.

Figure 11B shows the progressive development of the scCO<sub>2</sub> plume. A typical “gravity override” profile is seen to develop and persist after 1 year of injection, but caprock properties are such that scCO<sub>2</sub> leakage into the caprock is evident even after one year. By 5 years, some scCO<sub>2</sub> has been transported into the overlying aquifer. The presence of the conductive leaky well is evident in the asymmetry of the scCO<sub>2</sub> plume. The pressure dissipation surrounding the leaky well is such that the scCO<sub>2</sub> plume develops an asymmetry and has advanced more toward the leaky well than away from it after 5 years of injection. By 50 years, scCO<sub>2</sub> has begun to pond at the top of the aquifer, which by default is an impermeable boundary.

Leakage of NaCl and aqueous CO<sub>2</sub> into the caprock associated with injection is shown in Figure 11C and D. Little if any brine is seen to migrate into the aquifer after 50 years of injection, as most water displacement is to the sides of the reservoir domain or up the leaky well. However aqueous CO<sub>2</sub>, which attends the scCO<sub>2</sub> transport through the caprock, is quite evident in the aquifer after 5 years of injection. The heightened NaCl mass fraction near the wellbore is due to salt precipitation accompanying dryout of brine near the wellbore.

Figure 12 shows time series of pressure, scCO<sub>2</sub> Sg (saturation), aqueous CO<sub>2</sub>, and NaCl mass fraction at two cells during the injection simulation. Element 2121 (this is the TOUGH2-assigned cell name in the grid, shown in the blue curves) occurs just above the injection zone at the reservoir caprock boundary, while element 3551 (brown curves) occurs just above the injection zone at the caprock-aquifer boundary. Both cells experience a similar pulse of pressure increase following initiation of injection, which dissipates after about 10 years as the scCO<sub>2</sub> plume migrates to larger portions of the reservoir and leaks through the caprock. A similar rise in scCO<sub>2</sub> is seen in both cells, but a maximum in cell 3551 occurs and then levels off, presumably as the pressure levels off and scCO<sub>2</sub> spreads upward through the caprock and into the aquifer. From the time series of NaCl mass fraction for cell 3551, no brine has migrated upward from the injection well from injection.

This simple case illustrates the physics behind our leakage scenarios of leaky well and leaky caprock and is used for the coupled DAKOTA- TOUGH2 feasibility study discussed below. In order to minimize simulation times, for the DAKOTA realizations, we assume homogeneous reservoir properties, and will assume zero salinity throughout the simulation domain. These assumptions have little effect on the overall leakage realizations we investigate below.

Figure 11A

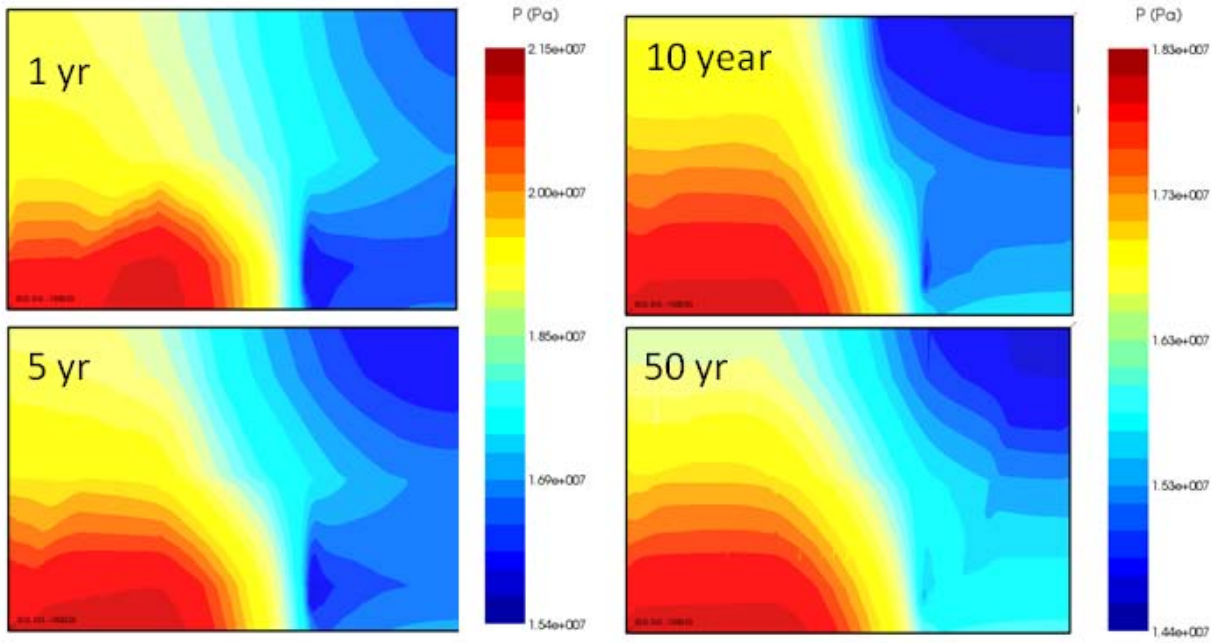


Figure 11B

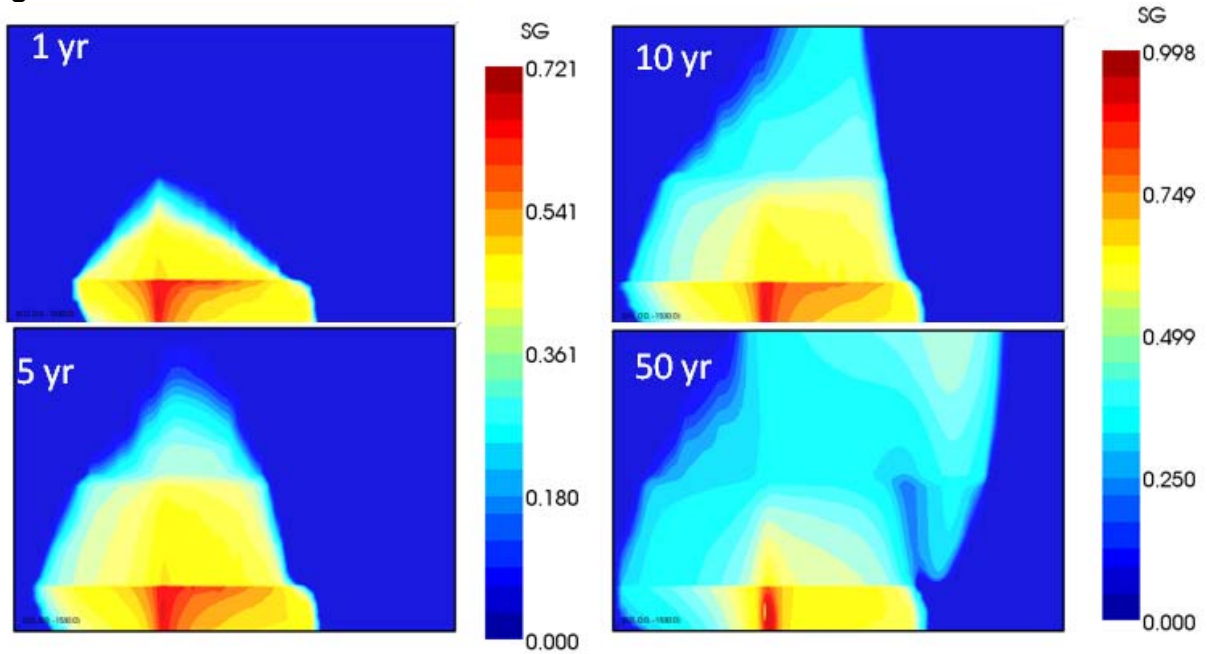


Figure 11C

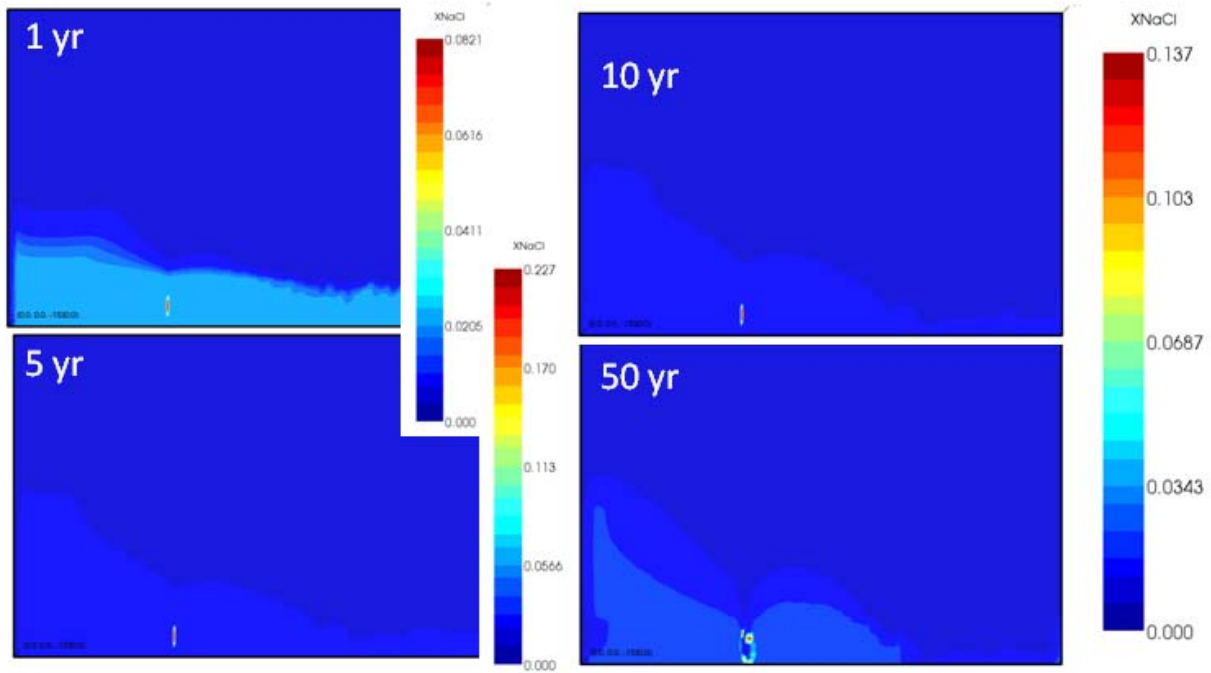
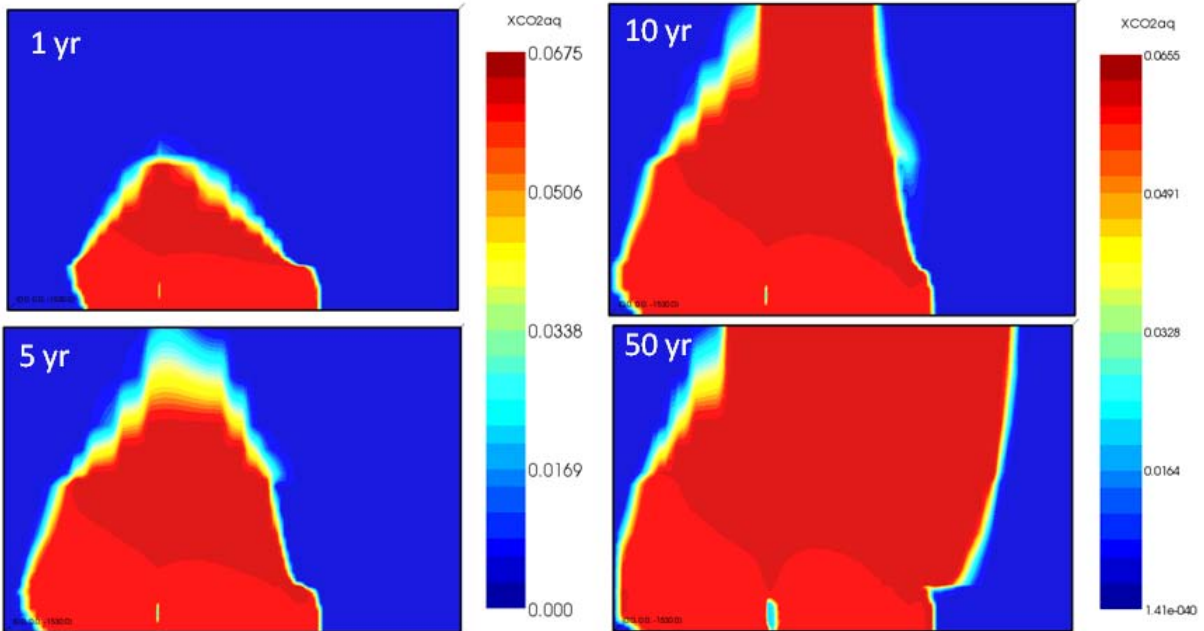
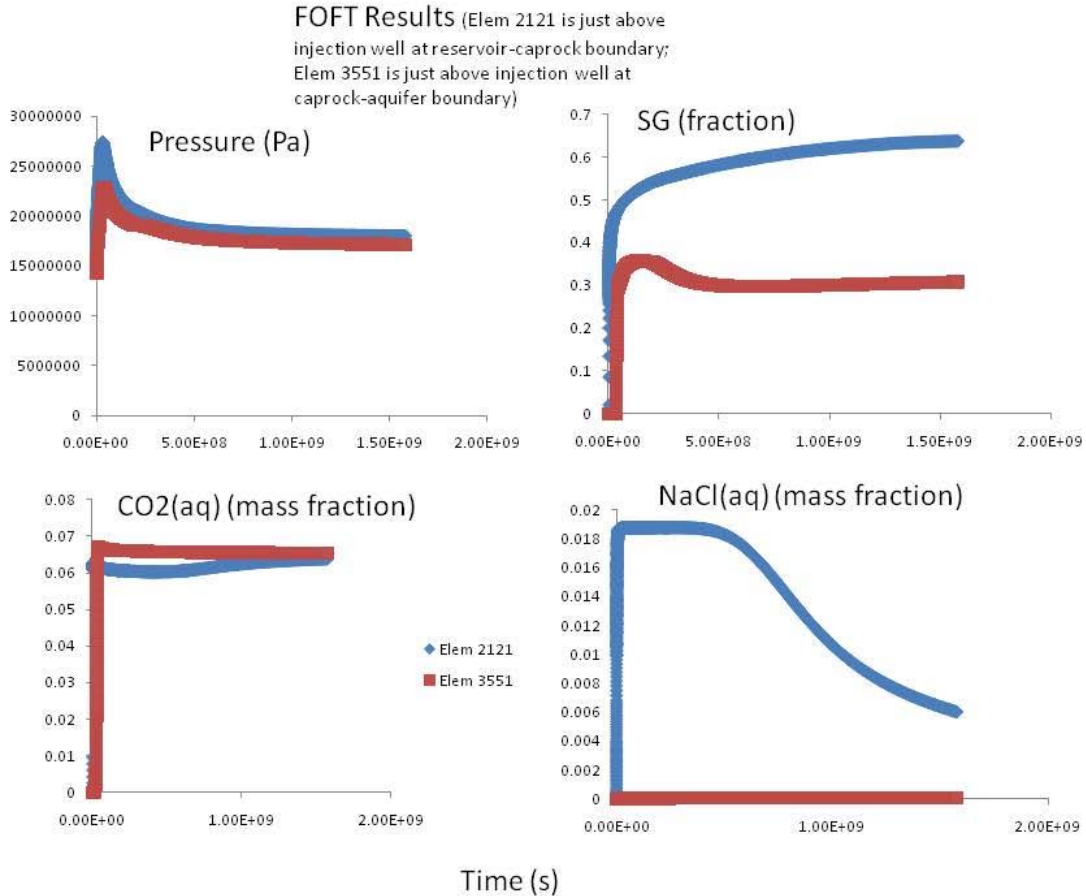


Figure 11D



**Figure 11.** Profiles with time of consequences of CO<sub>2</sub> injection using the mesh and model shown in Figure 7. A. Profiles of pressure (Pa) after 1, 5, 10, and 50 years of injection. B. Profiles of scCO<sub>2</sub> saturation after 1, 5, 10, and 50 years. C. Profiles of mass fraction of NaCl (both dissolved in aqueous solution and solid) after 1, 5, 10, and 50 years. The high NaCl amounts near the injection well are solid salt, due to dry-out associated with injection near the wellbore. D. Profiles of aqueous CO<sub>2</sub> after 1, 5, 10, and 50 years of injection.





**Figure 12.** Time series of pressure, scCO<sub>2</sub> saturation, aqueous CO<sub>2</sub> and mass fraction of NaCl for elements 2121 and 3551 in the TOUGH2 grid. Element 2121 occurs just above the injection well at the reservoir caprock boundary, while element 3551 occurs just above the injection well at the caprock-aquifer boundary.

### 5.3.2. Multiple realization case

The coupled DAKOTA- TOUGH2 system was run using sampled values of the five uncertain parameters specified in Table 3; injection rate, abandoned well productivity index, and caprock properties of permeability, porosity and residual liquid saturation. For this demonstration, twenty seven input vectors were developed and utilized in TOUGH2 simulations. In all cases a sampled constant amount of CO<sub>2</sub> is injected for a period of 30 years and the simulation is continued to a total time of 100 years to observe CO<sub>2</sub> movement in the injection zone and through the abandoned well and caprock. Key results from the twenty seven vectors are shown in Figures 13 to 19. Figures 13 and 14 show pressure and gas saturation results in an injection well model element (Element 821) located in the middle of a 5-element injection column. The horsetail plots of pressure and saturation for the twenty seven vectors show a spread in results, a direct effect of the range of sampled parameters. Pressure builds up rapidly in the injection well element and the surrounding elements as more CO<sub>2</sub> is injected and brine is pushed out. The increased CO<sub>2</sub> injection also results in increases in gas saturation. The magnitude of the increases depends primarily on the injection rate and to a lesser extent on the other sampled parameters. Thus,

vectors with low injection rates show lower pressure build-up. With time the pressure build-up decreases as the brine is pushed further and fluid moves to the abandoned well and the caprock, away from the injection well. Use of a homogeneous reservoir with a permeability of  $1.94 \times 10^{-13} \text{ m}^2$  also facilitated movement of fluid away from the injection well. Higher gas saturations in the injection well were maintained by high capillary pressure conditions. When the capillary pressure in the injection well element reaches the maximum specified (i.e.  $2 \times 10^7 \text{ Pa}$  in the reservoir) brine flow into the element is reduced, and thus high gas saturations are maintained.

Figures 15 to 17 show results of pressure, gas saturation and  $\text{CO}_2$  leakage in an abandoned well element (Element 1782) located in the middle of a 6-element column. Pressure and gas saturation build-up occur early, as a result of fluid ( $\text{CO}_2$  and brine) movement into the abandoned well. The build-ups occur at a delayed time when compared to the injection well, as the injection effects are felt in the abandoned well. The build-up in pressure and saturation at the abandoned well also resulted in increased  $\text{CO}_2$  leakage. As shown in Figure 17, leakage increases until around 30 years, when the  $\text{CO}_2$  injection is stopped. To evaluate the amount of leakage the Deliverability model of TOUGH2 was utilized. According to the Deliverability model the amount of leakage (liquid and gas) is a function of pressure difference between the reservoir pressure in the selected element and a specified flowing bottom hole pressure, productivity index and relative permeability. For this exercise the bottom hole flowing pressure was selected to be equal to the hydrostatic pressure at the element, while the productivity index was sampled as shown in Table 3. The variation in the magnitude of leakage in Figure 17 depends on the sampled values of the uncertain parameters, including the productivity index. The peak leakage rate is a big portion of the total injection rate, indicating that for this exercise the abandoned well is a major conduit for  $\text{CO}_2$  migration. In a more realistic setting the heterogeneity in the host rock and the caprock, and conditions of the abandoned well would control fast migration. A finer meshing would also provide more accurate results. Also, note the time step selection in the simulations leads to discrete, rather than continuous results. This could be mitigated with more refined time-stepping.

The  $\text{CO}_2$  also migrates to the cap rock overlaying the reservoir and to the aquifer above it. The mass balance of  $\text{CO}_2$  in the three modeled materials (rock types) provides the total amount of  $\text{CO}_2$  that migrated to the caprock and the aquifer. Migration patterns at specific locations can be studied by plotting fluxes at specific element boundaries. Figures 18 and 19 show gas flux or flowrate versus time plots for the 27 vectors, at two selected locations representing the reservoir-caprock boundary and the caprock-aquifer boundary. [Note: Figures 20 to 23 provide the total extent of  $\text{CO}_2$  movement to the caprock and the aquifer over 100 years.] The selected element boundaries are located on the same column as the injection well, shown in Figure 10 designated as FOFT cells. Figure 18 shows movement of gas from the reservoir to the cap rock during the 30-year injection period, with a small amount of reverse flow after 30 years. Figure 19 provides the same trend as in Figure 18.

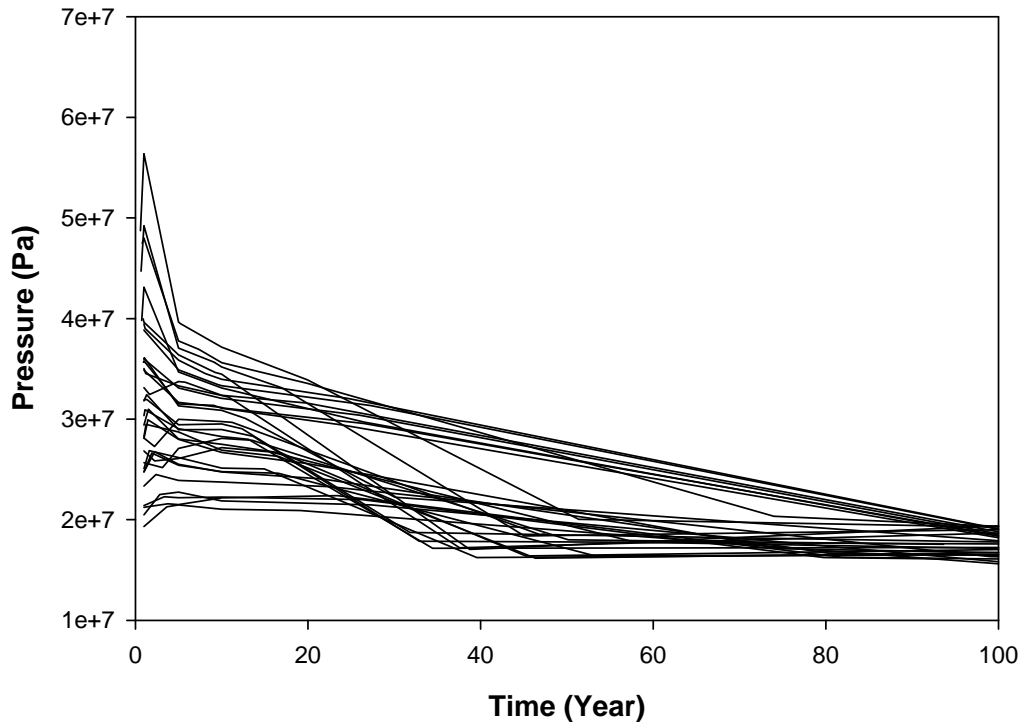


**Figure 13.** Pressure in Injection Well (Element 821) –27 Vectors

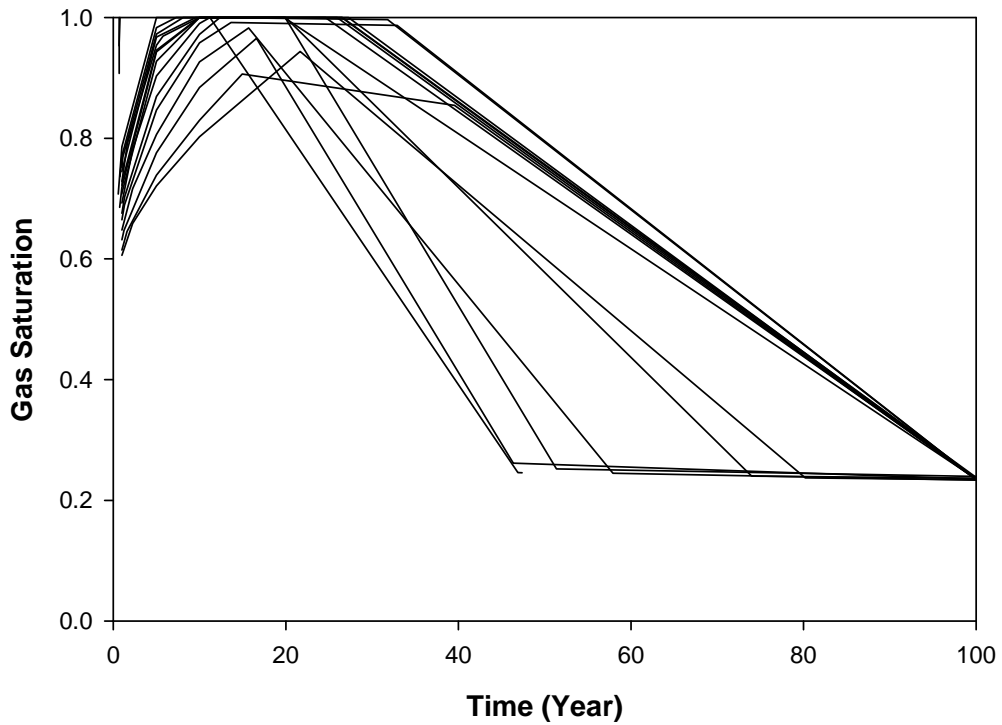


**Figure 14.** Gas Saturation in Injection Well (Element 821) –27 Vectors

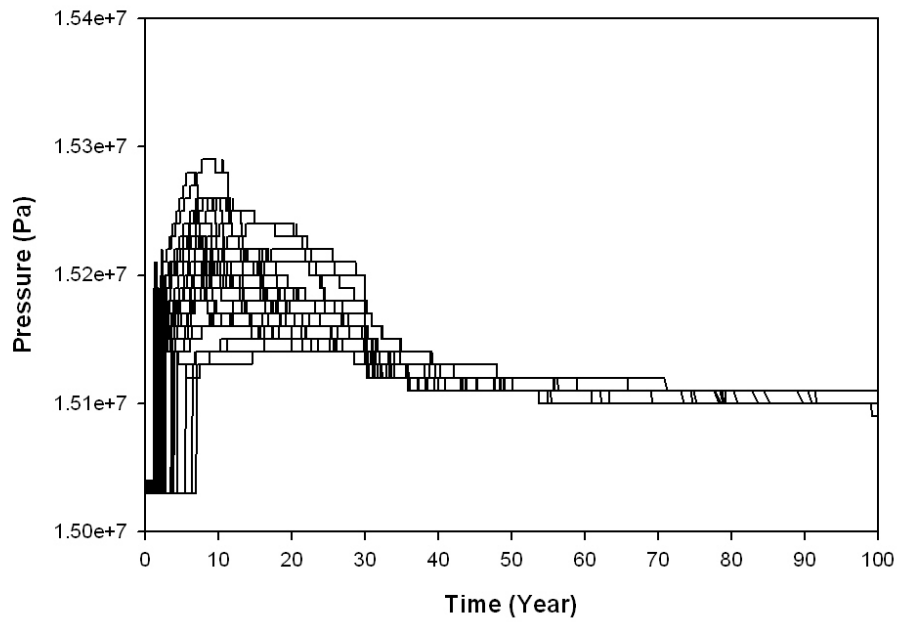


**Figure 15.** Pressure in Abandoned Well (Element 1782) –27 Vectors. Discrete appearance of the curves are due to the limited number of model output data points.

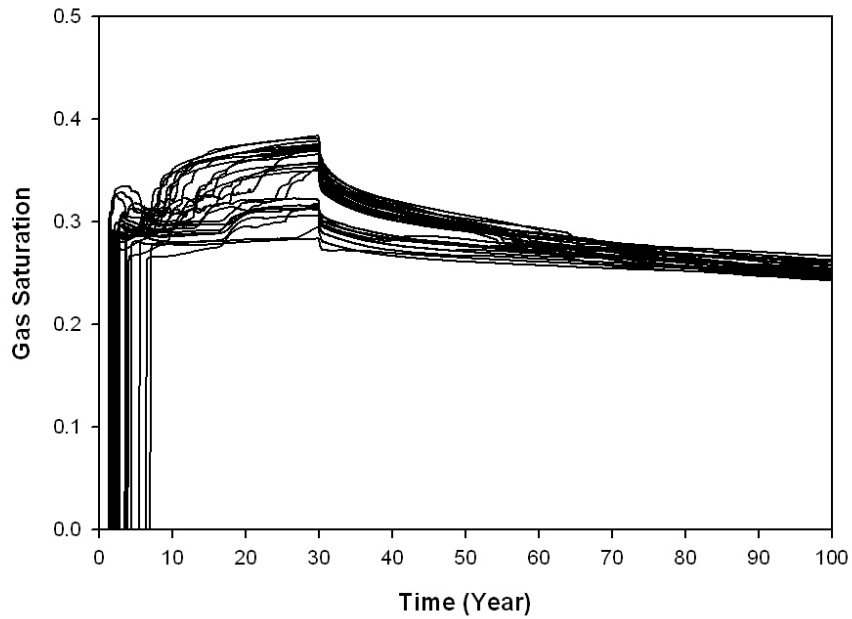


**Figure 16.** Gas Saturation in Abandoned Well (Element 1782) – 27 Vectors

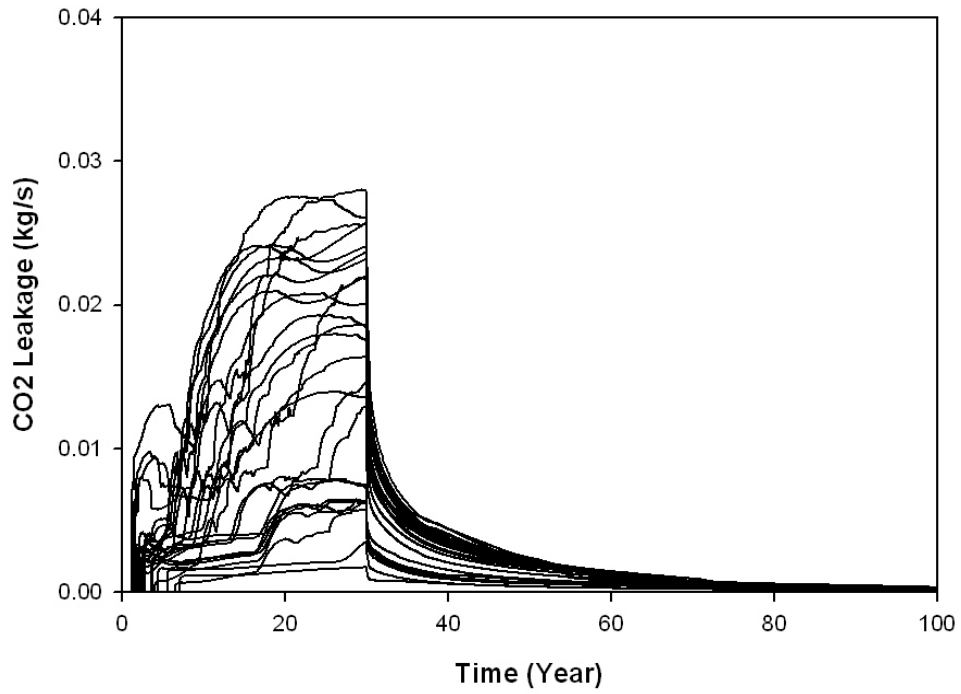


**Figure 17.** CO<sub>2</sub> Leakage from Abandoned Well (Element 1782) – 27 Vectors

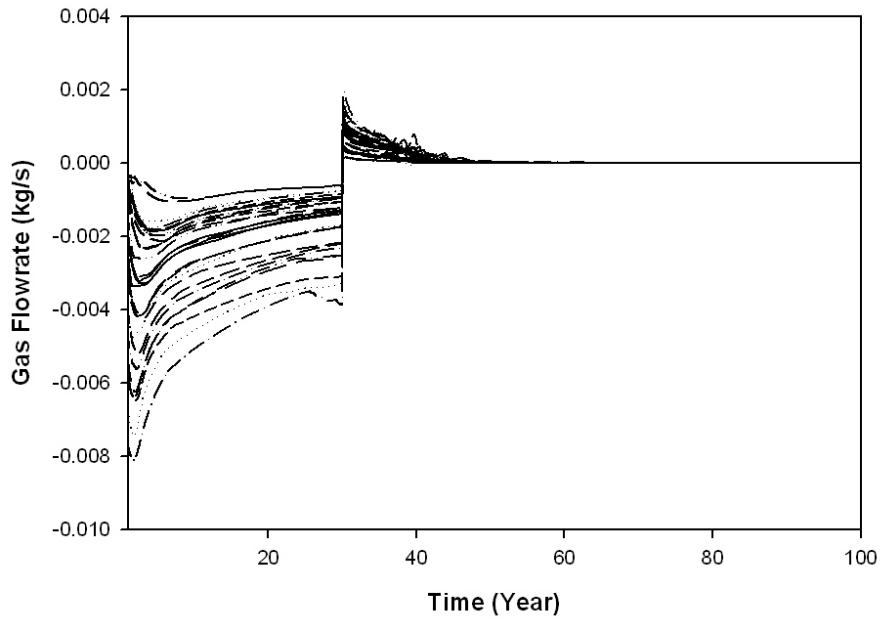


**Figure 18.** Gas Flowrate at the Reservoir-Caprock Boundary (Element 1991 to Element 2121) – 27 Vectors. (Negative flowrate indicates flow from reservoir to caprock)

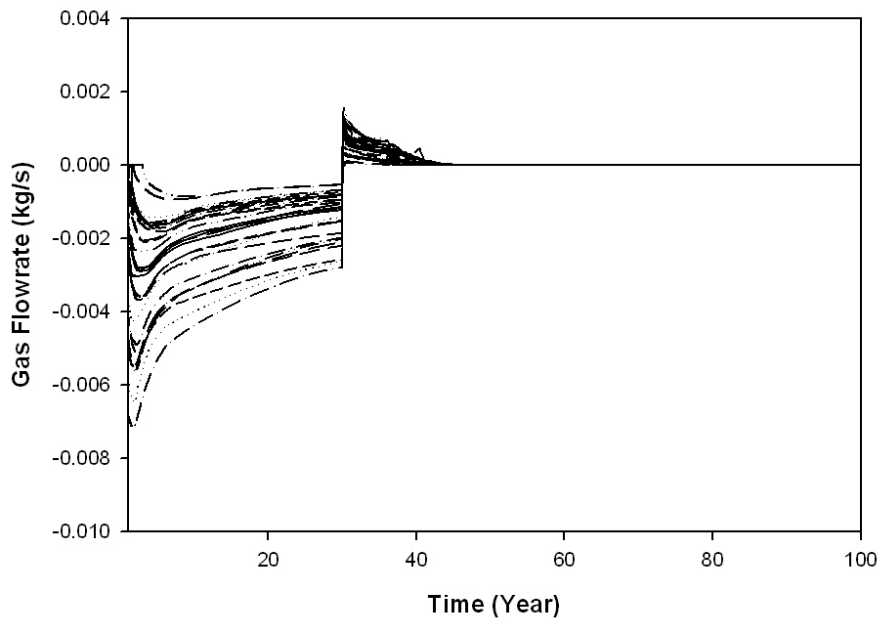


**Figure 19.** Gas Flowrate at the Caprock-Aquifer Boundary (Element 3421 to Element 3551) – 27 Vectors. (Negative flowrate indicates flow from caprock to aquifer)

#### 5.4. Uncertainty Quantification and Sensitivity Analysis

The system for storage of carbon dioxide in the subsurface has potentially large uncertainties in the material properties of the storage area, as well as in the measurements taken to attempt to characterize the subsurface. Heterogeneous geologic materials are ubiquitous in such systems. The degree of uncertainty varies from site to site, as some have been investigated more thoroughly than others (e.g., existing oil and gas reservoirs), and some are more homogeneous in their material properties than others. There are a number of methods to support quantification of uncertainty. This quantification can provide a measure of how reliable or accurate results are for a given carbon storage scenario.

As an example of uncertainty quantification, concentrations of carbon dioxide in caprock and aquifer are important metrics for evaluating the extent of leakage and thermodynamic balances. Mass of CO<sub>2</sub> appearing in either gaseous or aqueous phase is used as DAKOTA's response functions. Figures 20 to 23 show the cumulative distribution functions of resulting CO<sub>2</sub> concentrations based on the sampled parameter vectors. The total CO<sub>2</sub> in the gas phase within the overlying aquifer spans almost two orders of magnitude from 1x10<sup>5</sup> to 3.5x10<sup>7</sup> kilograms, while the total CO<sub>2</sub> dissolved in aqueous phase varies only by a factor of approximately 2 from one sampling point to another. The amount of dissolved carbon dioxide in the overlying aquifer varies from approximately 1.6x10<sup>7</sup> to 2.6x10<sup>7</sup> kilograms after 100 years. The two phases combined yield a substantial presence of carbon dioxide. Lesser amounts of CO<sub>2</sub> appear in both phases within the caprock compared to the injection aquifer after 100 years. The mean values of CO<sub>2</sub> mass within the caprock are 1.75x10<sup>6</sup> kilogram in the gas phase and 1.1x10<sup>6</sup> kilogram in the dissolved phase.

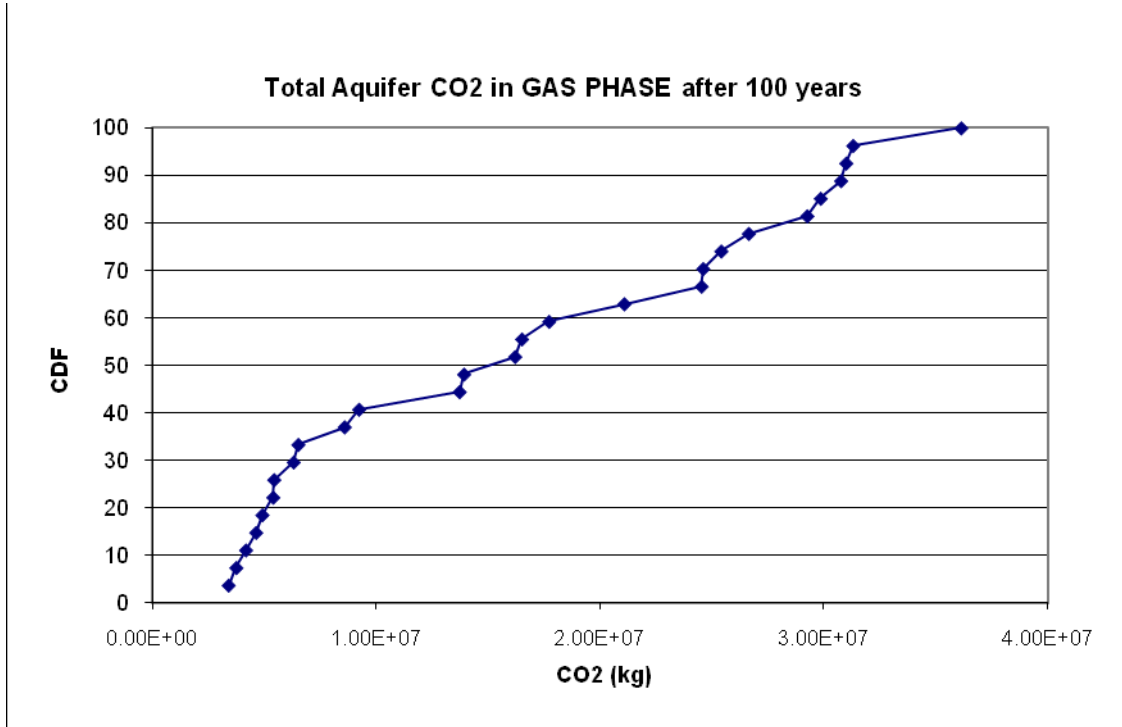


**Figure 20.** Total amount of carbon dioxide in gas phase within the overlying aquifer after 100 years.

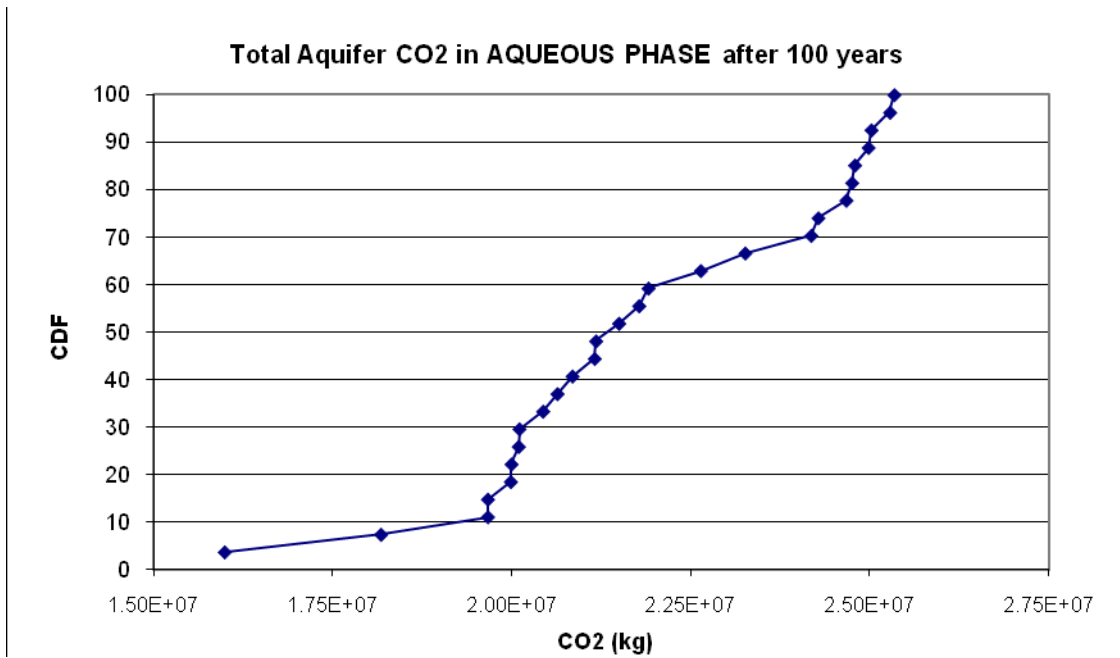


**Figure 21.** Total amount of dissolved carbon dioxide in aqueous phase within the overlying aquifer after 100 years.

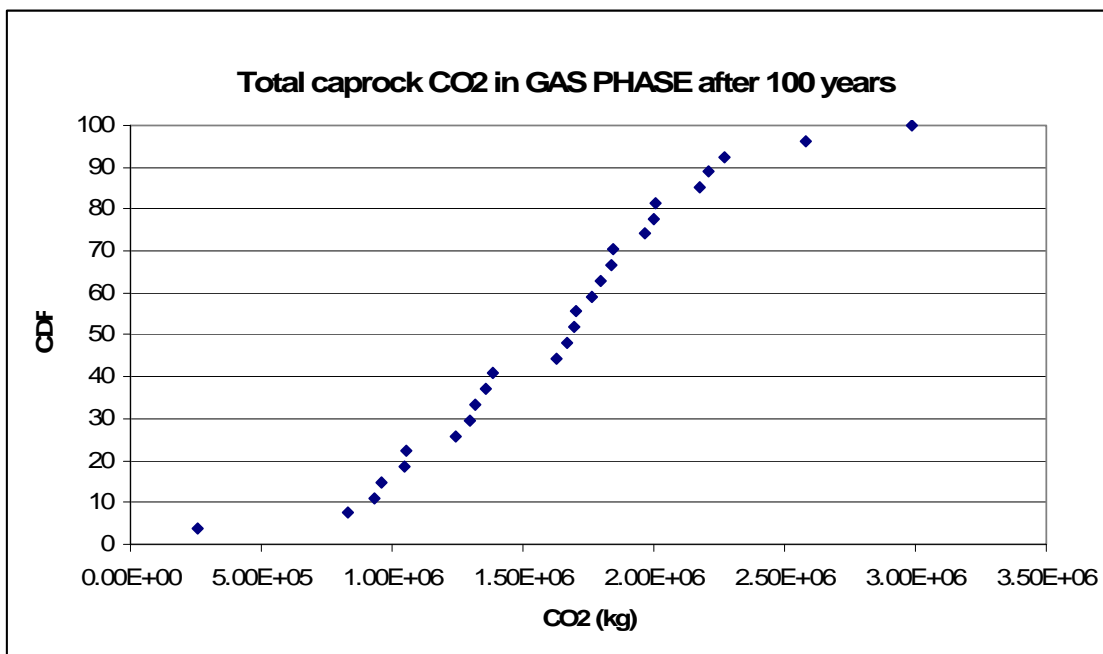


**Figure 22.** Total amount of carbon dioxide in gas phase within caprock after 100 years

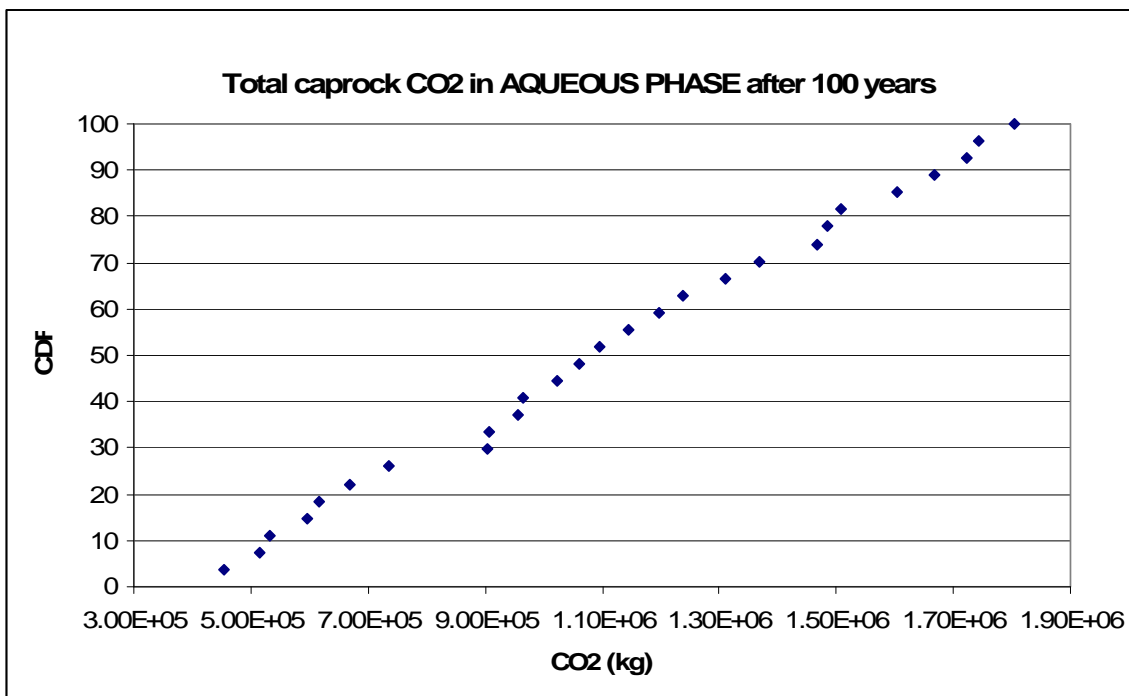


**Figure 23.** Total amount of dissolved carbon dioxide in aqueous phase within caprock after 100 years.



In addition to checking CO<sub>2</sub> quantities in the caprock and overlying aquifer, the amount of CO<sub>2</sub> in the host rock is assessed. Figures 24 and 25 show cumulative distribution functions of carbon dioxide within the reservoir in gas and aqueous phases, respectively, after 100 years. Total CO<sub>2</sub> varies from 4.5x10<sup>6</sup> to 5.7x10<sup>6</sup> kilogram in the gas phase while the total mass varies from 2.0x10<sup>6</sup> to 1.4x10<sup>7</sup> in the aqueous phase. For this initial prototype case, the results indicate the injected CO<sub>2</sub> is not remaining in the injection zone.

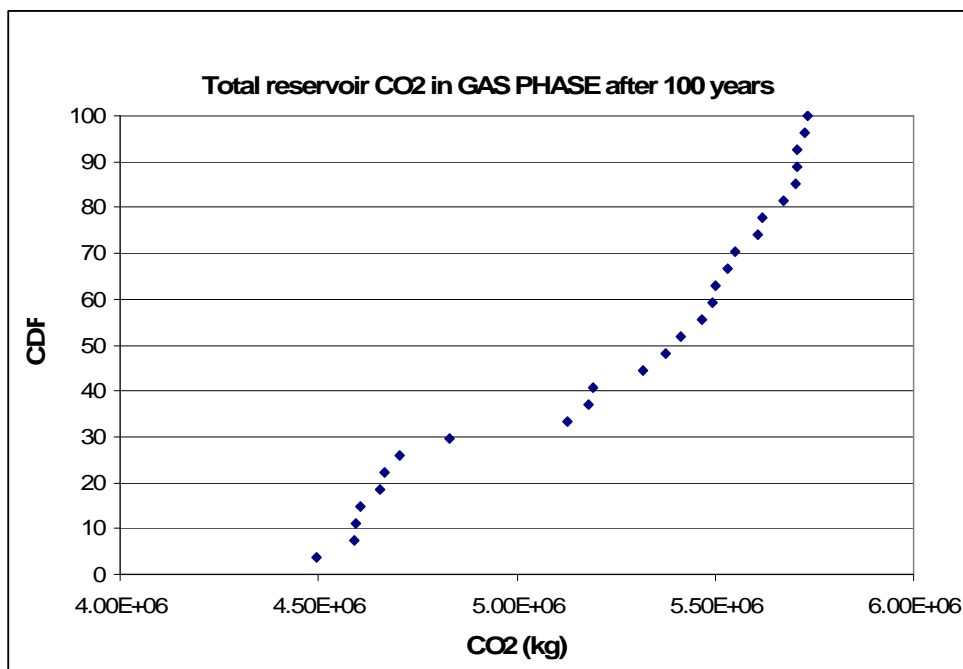
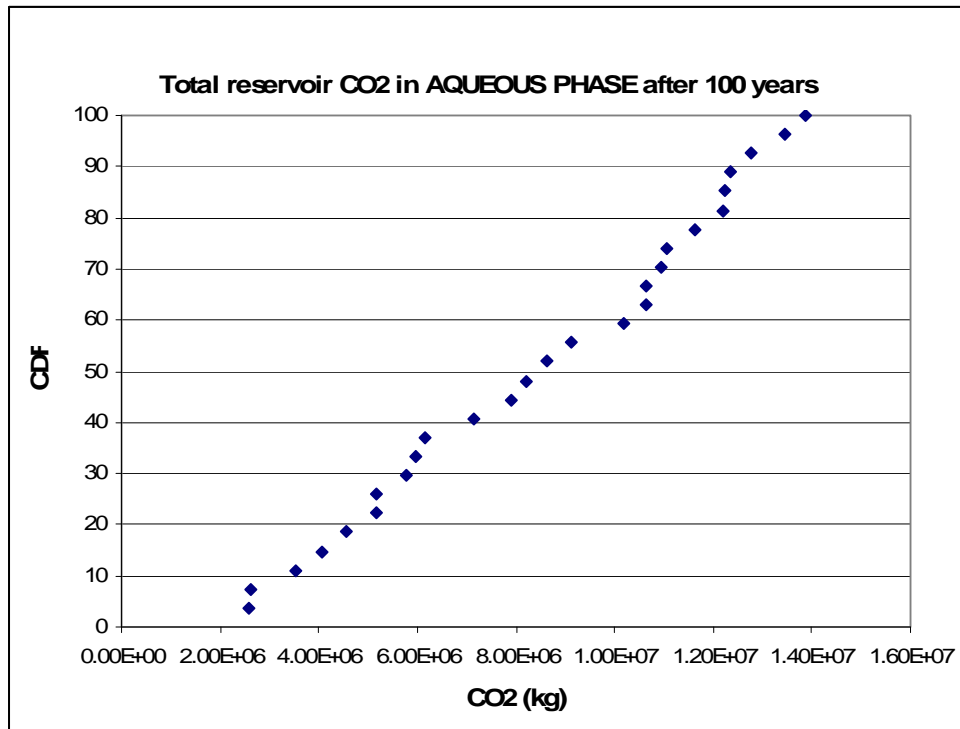


Figure 24. Total amount carbon dioxide in gas phase within reservoir after 100 years.



**Figure 25. Total amount of dissolved carbon dioxide in aqueous phase within reservoir after 100 years.**

The results from multiple PA realizations also allow us to perform sensitivity analysis through variable correlation to identify the important model input parameters for CS performance. To check for correlations between input parameters and the amount of carbon dioxide present in the reservoir, the parameter values are plotted against total amounts of CO<sub>2</sub> in gas and in aqueous phases. Graphs of caprock properties (porosity, permeability, and residual water saturation), injection rate, and productivity index versus aqueous CO<sub>2</sub> mass are shown in Figures 26 to 30 respectively. Other than the injection rate, there are no visible correlations between dissolved CO<sub>2</sub> in the aqueous phase and caprock porosity, caprock permeability, and caprock residual water saturation. Moreover, there is no correlation between productivity index and dissolved CO<sub>2</sub> in the aqueous phase. However, the correlation is high between the injection rate and dissolved CO<sub>2</sub> in the aqueous phase. This stronger correlation is expected since the injection rate directly impacts the amount of CO<sub>2</sub> entering the reservoir.

Graphs of caprock properties (porosity, permeability, and residual water saturation), injection rate, and productivity index versus CO<sub>2</sub> mass in the gas phase are shown in Figures 31 through 35, respectively. Other than the injection rate, there are no visible correlations between gaseous CO<sub>2</sub> in the reservoir and caprock porosity, caprock permeability, and caprock residual water saturation. Similarly, there is no correlation between productivity index and gaseous CO<sub>2</sub> in the reservoir domain. As depicted in Figure 34, the correlation is less pronounced between the injection rate and CO<sub>2</sub> in the gas phase at low injection rates in the range of 0.01 through approximately 0.025 kg/s. Additional analysis is needed to clarify this effect. The effect of low and high injection rates is also evident in Figures 33 and 35 where two distinct “bands” of data

can be discerned. In Figure 33, larger values for gaseous mass of CO<sub>2</sub> correspond to higher injection rates. Thus, the correlation with caprock residual water saturation is not evident as the correlation with injection dominates. However, at lower injection rates, a trend is observed where higher caprock residual saturation would correspond to lower brine mobility in the caprock, and therefore, higher CO<sub>2</sub> gas mobility. This would lead to higher CO<sub>2</sub> migration into the caprock, and reduced gaseous CO<sub>2</sub> mass in the reservoir. Figure 35 also indicates the data “band” separation for the lower and higher injection rates. However, any meaningful correlation at these injection rates is not evident because of the narrow range of productivity index selected for this problem.

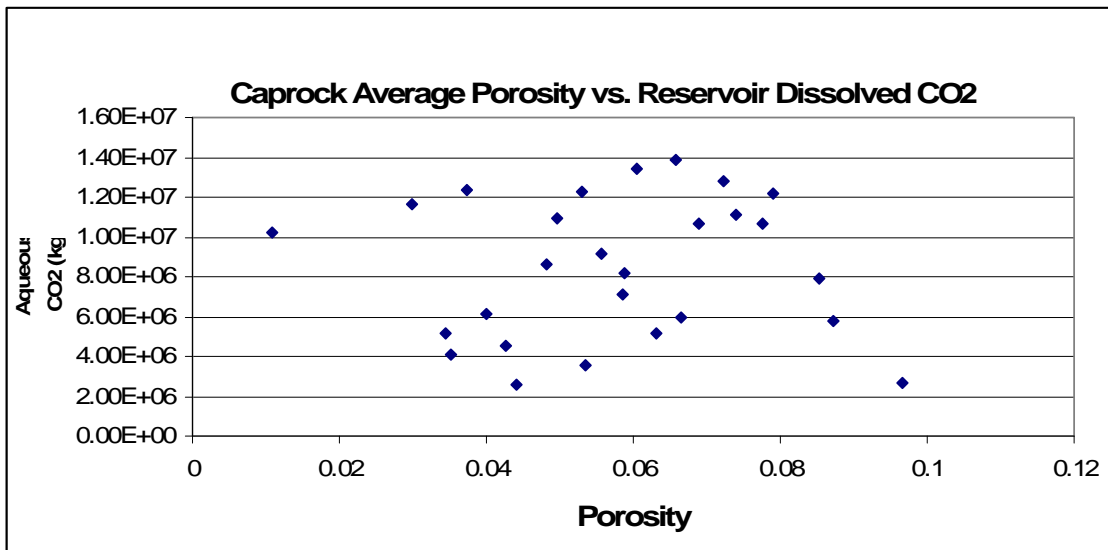


Figure 26. Sampled porosity values versus total dissolved CO<sub>2</sub> within the reservoir after 100 years.

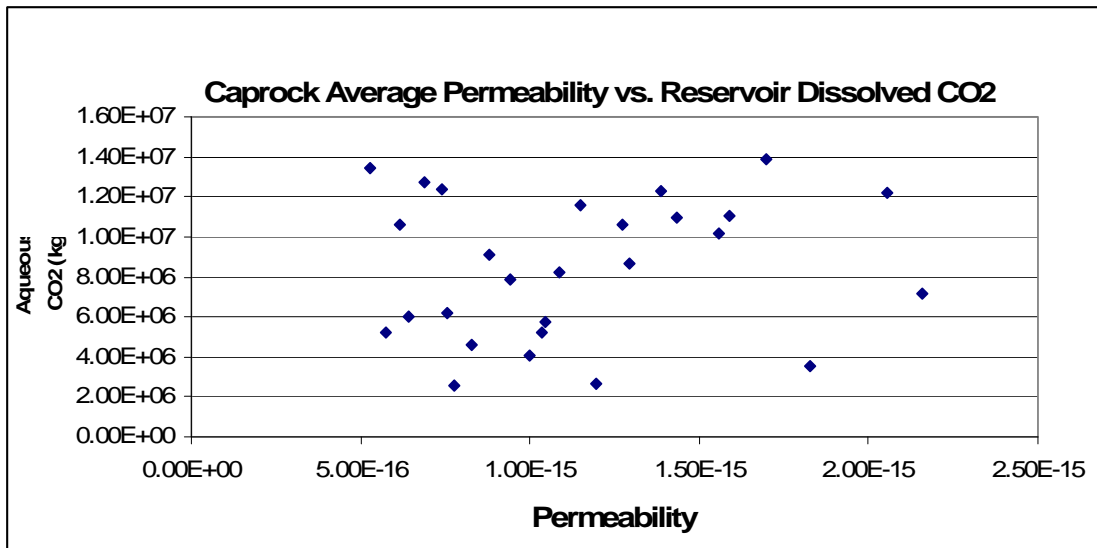
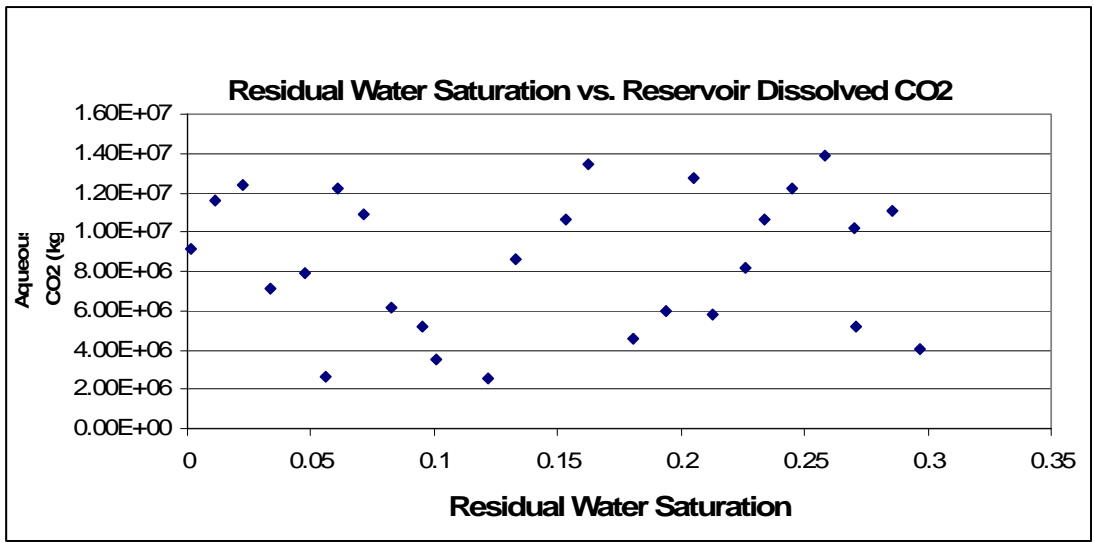
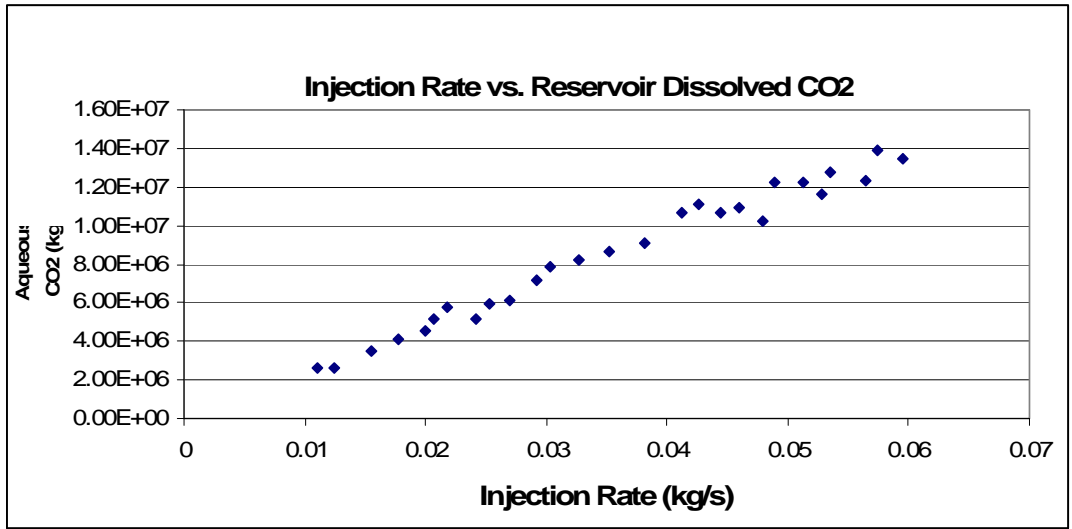


Figure 27. Sampled permeability values versus total dissolved CO<sub>2</sub> within the reservoir after 100 years.



**Figure 28. Sampled residual water saturation versus total dissolved CO<sub>2</sub> within the reservoir after 100 years.**



**Figure 29. Sampled injection rates versus total dissolved CO<sub>2</sub> within the reservoir after 100 years.**

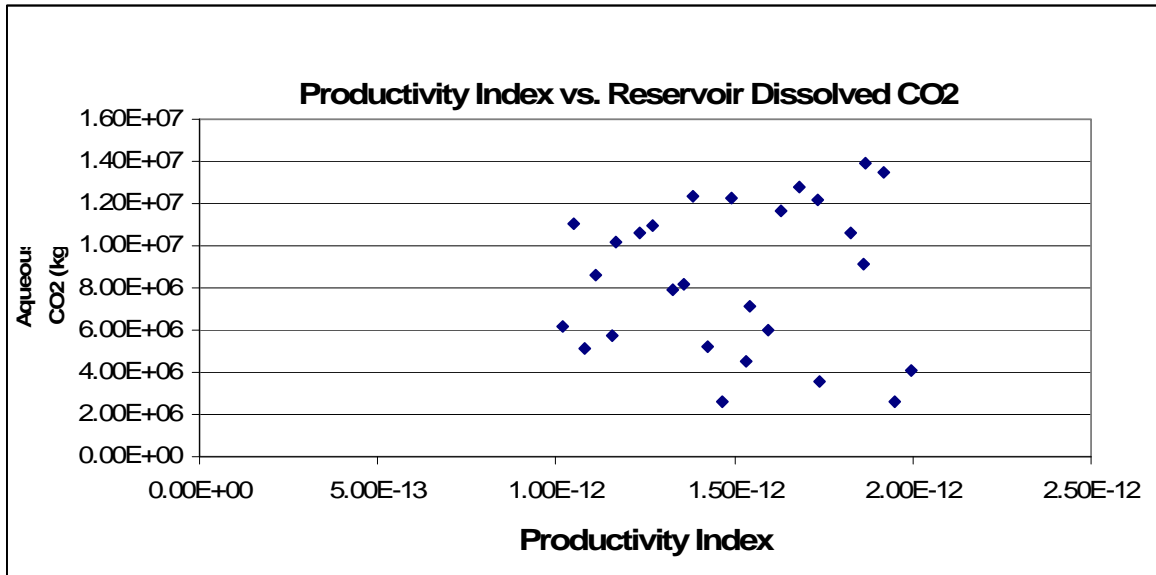


Figure 30. Sampled productivity indices versus total dissolved CO<sub>2</sub> within the reservoir after 100 years.

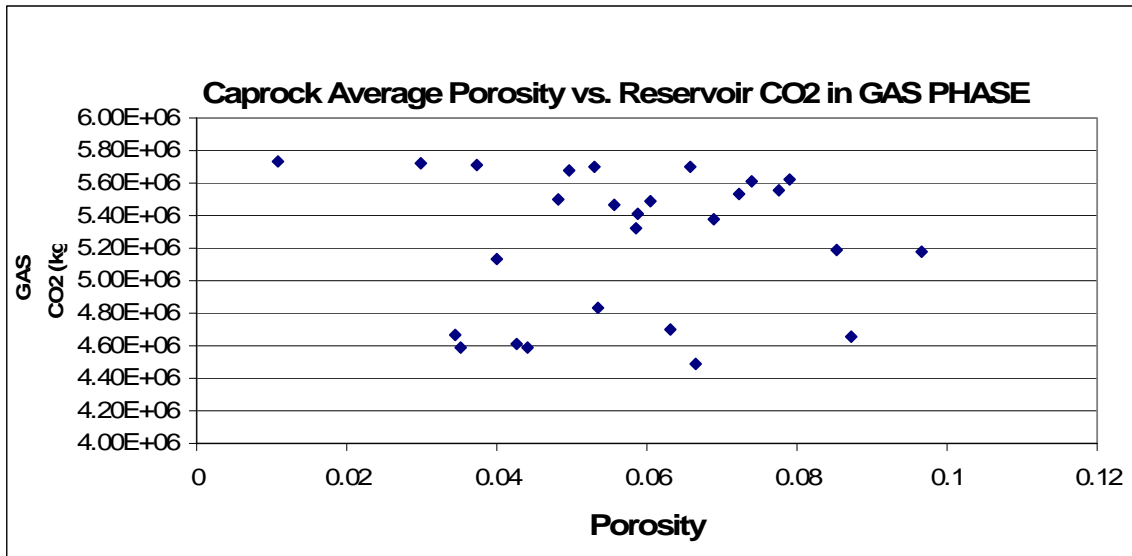


Figure 31. Sampled porosity values versus total gas-phase CO<sub>2</sub> within the reservoir after 100 years.

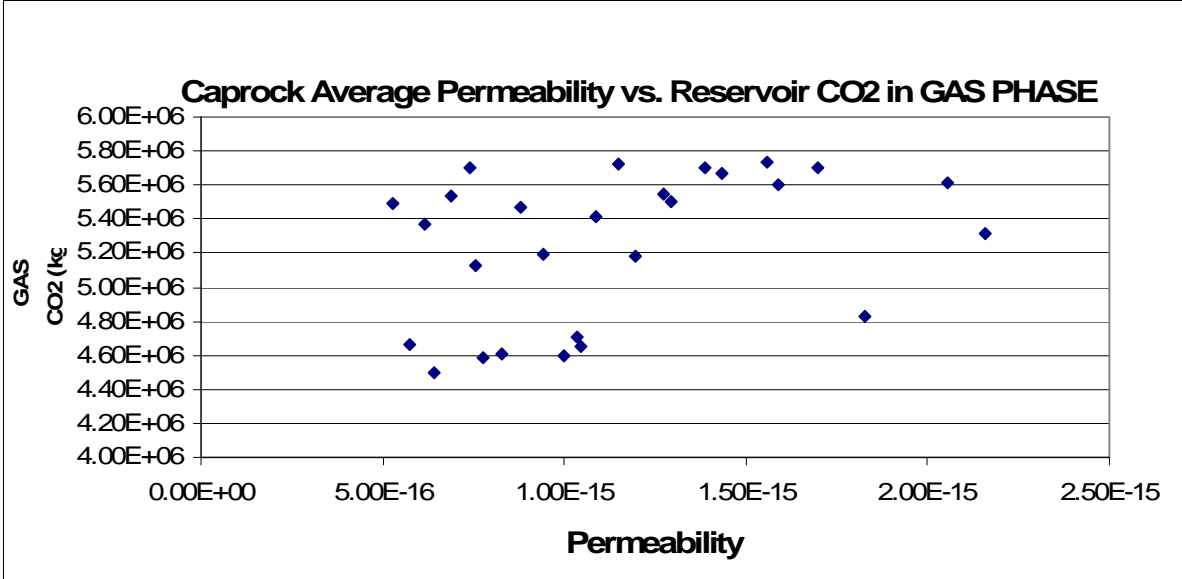


Figure 32. Sampled permeability values versus total gas-phase CO<sub>2</sub> within the reservoir after 100 years.

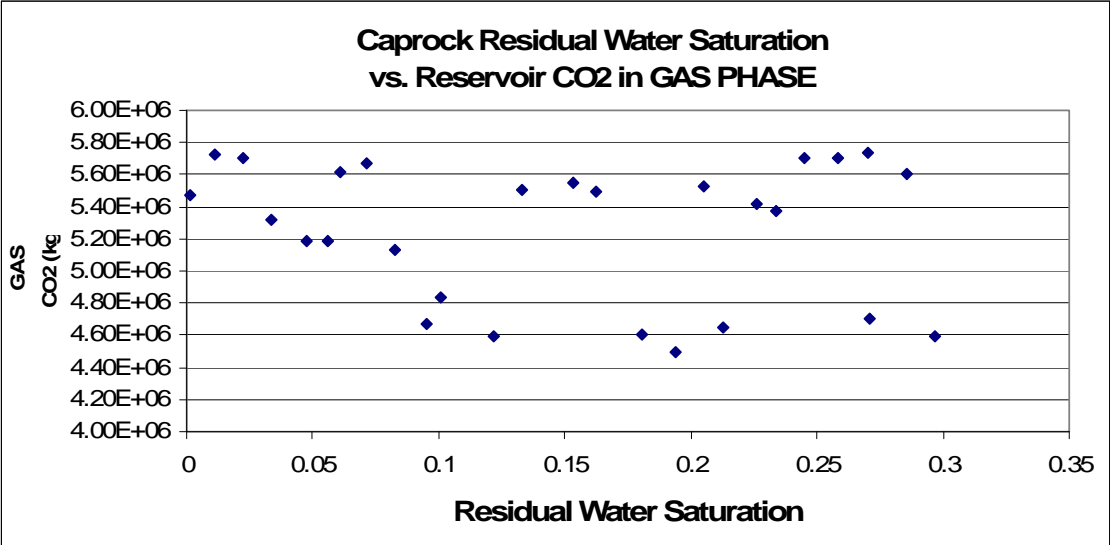


Figure 33. Sampled residual water saturation versus total gas-phase CO<sub>2</sub> within the reservoir after 100 years.

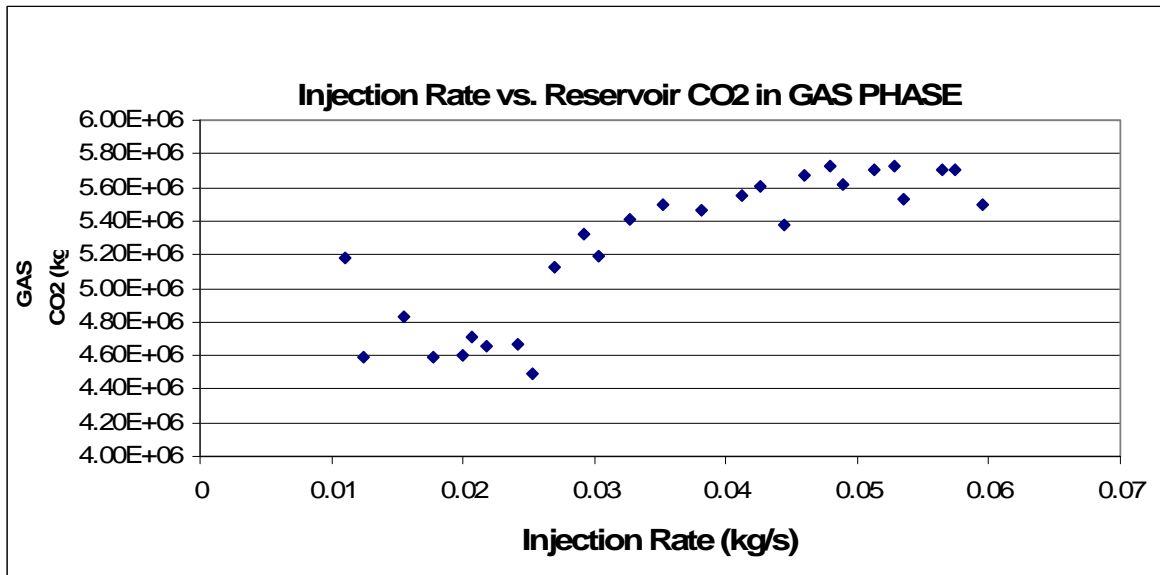


Figure 34. Sampled injection rates versus total gas-phase CO<sub>2</sub> within the reservoir after 100 years.

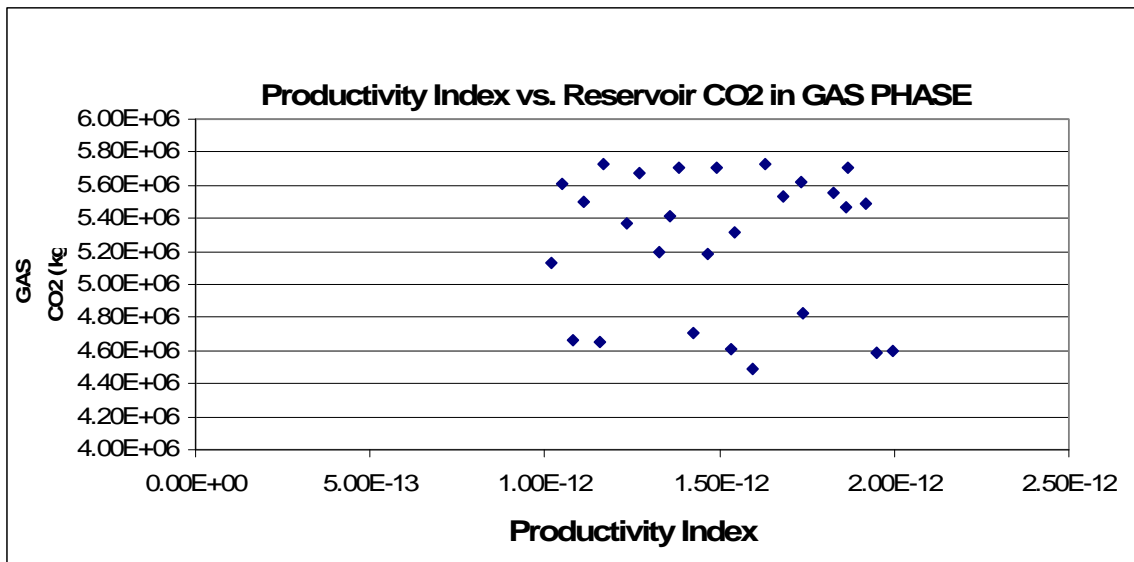


Figure 35. Sampled productivity indices versus total gas-phase CO<sub>2</sub> within the reservoir after 100 years.

## 6. DESCRIPTION OF OPTIMIZATION APPROACH

Because of time constraint, we have demonstrated the capability of the EPAS for its forward PA calculations but not for its inverse model part. Since we have successfully demonstrated the use of DAKOTA as the PA driver of the EPAS (see Section 3), the inverse model part can readily be demonstrated with the built-in optimization capability in DAKOTA. Such demonstration will be part of future work. To fully utilize the capabilities for optimization within DAKOTA, a conceptualization of the system was developed including high level parameters for major components of the system. The selection of these optimization metrics and the overall approach to optimize the system performance is described below.

### 6.1. Selection of Optimization Metrics

There are a number of issues arising from recent complex systems (both controlled and uncontrolled) that may support the effort to minimize the cost and the risk, while optimizing the injection of carbon dioxide. The overall carbon storage system has a top-level set of metrics to be optimized. These include the maximum injection rate, the acceptable formation pressure, minimum level of leakage of the injected carbon dioxide, and overall cost of the system. For the cost component, such things as the number of injection wells, the number of downhole and surface sensors to detect both pressure and leakage, and the appropriate timing of satellite data collection to evaluate surface elevation changes and leakage. The primary objective is high performance accuracy and reliability in an uncontrolled and uncertain environment.

### 6.2. Detailed Optimization of Carbon Sequestration System

The initial effort to optimize the carbon storage system involved assessing the key system parameters as described in Section 3. There were a number of natural system parameters, as well as the engineered system parameters for the injection well and its operation. The cost parameters were not included in the optimization of the system, though they clearly are important if the subsurface carbon storage approach is to be a significant benefit in the reduction of carbon dioxide emissions.

The initial effort provided some useful lessons applicable to future scaleup of these analyses. The computational power required for codes such as TOUGH2 and DAKOTA is significant, and may be a key to the future applicability of the tools. The concept of a desktop assessment may not be feasible in real time, due to the processor and memory requirements of the analyses, especially when we consider larger data streams and more injection/leakage wells. We used a simple structured grid for this analysis, and unstructured or Voronoi meshes could be applied for more efficient numerical strategies. Linkage of TOUGH2 and DAKOTA was not a seamless process either, indicating there may need to be some development on the interface with other process models if the substantial capability of the DAKOTA toolset are to be further utilized for subsurface carbon storage analyses.



### 6.3. Fusion of Modeling with Carbon Data

There are a number of carbon sequestration or injection projects ongoing both in the U.S. and internationally. Figure 36 shows the location of projects in the U.S. (NETL, 2010b). There are several significant international projects often cited as examples of successful injection projects, including Weyburn in Canada (NETL, 2010c), Sleipner in the North Sea, and In Salah in Algeria (EPA, 2010). These projects are producing significant data for analysis and potential inclusion into models to support enhanced predictive capability. To appropriately incorporate this large amount of data, applicability to the model, and appropriateness for updating the model, the inverse model capability developed in the EPA PAS would be useful. This effort would be conducted in future phases of the development of the PA capability.

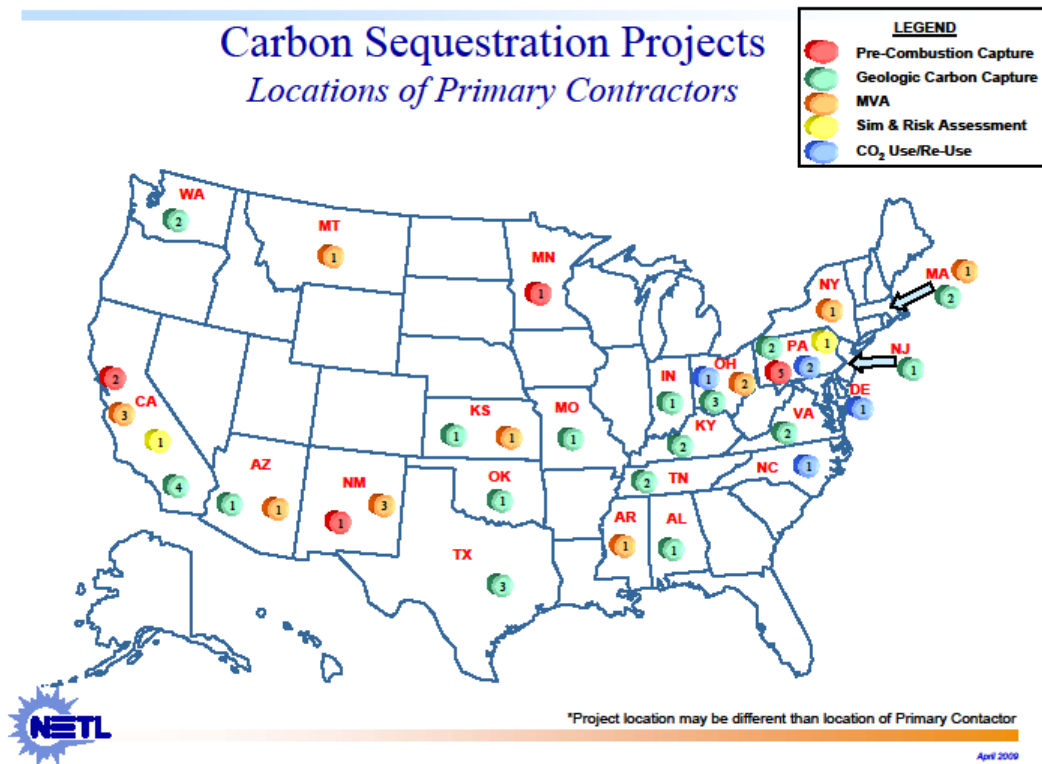


Figure 36. Map of Carbon Sequestration Projects in U.S. (NETL, 2010b)

### 6.4. Management Tools for Prioritization of Carbon Sequestration Program

To be useful for management decision making, the approach needs to be able to be conducted rapidly, with capability to conduct sensitivity analyses for parameters perceived important, have useful visualization capabilities, and properly optimize the system. As noted previously, some of the key parameters to be optimized include the overall injection scheme (volumes, timing, number of injection points, etc), the cost evaluation/investment evaluation scenario. The injection scheme will necessarily include the uncertainties of the host formation.

## 7. SUMMARY AND FOLLOW-ON WORK

Under the support of Laboratory-Directed Research & Development (LDRD), a late-start LDRD project was initiated in June of Fiscal Year 2010 to explore the concept of an enhanced performance assessment system (EPAS) for carbon sequestration and storage. In spite of the tight time constraints, significant progress has been made on the project: (1) Following the general PA methodology, a preliminary Feature, Event, and Process (FEP) analysis was performed for a hypothetical CS system. Through this FEP analysis, relevant scenarios for CO<sub>2</sub> release were defined. (2) A prototype of EPAS was developed by wrapping an existing multi-phase, multi-component reservoir simulator (TROUGH2) with an uncertainty quantification and optimization code (DAKOTA). (3) For demonstration, a probabilistic PA analysis was successfully performed for a hypothetical CS system based on an existing project in a brine-bearing sandstone. The work lays the foundation for the development of a new generation of PA tools for effective management of CS activities.

During the conduct of the research provided herein, there were a number of areas that were determined to be of interest in development of the enhanced performance assessment capability for these systems (see Table 5).

The direct integration of multiple sensors, both land and satellite based, into an adaptive integrating modeling system is one of these areas. So-called data fusion would be a useful addition to the toolkit for these analyses. Data fusion involves the combination of data from multiple sources into a structure to deliver inferences or meaning that is more efficient and accurate than if looking at a single source of information. For example, pressure monitoring from CO<sub>2</sub> injection wells could be combined with satellite land surface monitoring to evaluate potential areas to highlight CO<sub>2</sub> monitoring looking for potential releases. Adaptive modeling and mesh or parameter refinement could also utilize the updated pressure information to further calibrate the site CO<sub>2</sub> model. The time scale for such analysis and updating would be dependent on site and injection characteristics.

The scenarios evaluated in this project were limited due to time constraints. However, the modeling and simulation structure has been established to conduct extensive scenario analysis with alternative conceptualizations (e.g. leakage possibilities), and cost evaluations. Some of these alternative conceptualizations were listed in Section 2. The scenarios can be tailored to be dependent on the generic or specific storage site under consideration.

Optimization of the key parameters in the carbon storage system was also constrained by the time allotted for the late start LDRD. There are a number of additional tools within the DAKOTA framework that could be exercised to evaluate the optimal solution for key parameters in the carbon storage system.

DAKOTA contains a large number of capabilities. The research conducted herein pointed out the need for some specialized additions to the DAKOTA framework to support the conduct of assessing the carbon storage systems.

**Table 5. Summary of Follow-on Work to Further this Research**

<b>Activity</b>	<b>Description of workscope</b>	<b>Estimated level of effort</b>
Refinement of FEP analysis	Additional evaluation and model development for FEPs not currently included	4-6 man months
Data Fusion	Develop linkage to various data sources to provide rapid updating of site carbon storage models	3-6 man months
Additional scenarios	Develop and conduct additional scenarios for analysis of the performance assessment technology	2-4 man months
Additional optimization	Utilize the full breadth of the DAKOTA toolkit for optimization of the key parameters of the carbon storage system	2-4 man months
Additional development of DAKOTA	Update DAKOTA for PA specific requirements	1-3 man months

## 8. REFERENCES

- Adams, B. M., Bohnhoff, W. J., Dalbey, K. R., Eddy, J. P., Eldred, M. S., Gay, D. M., Haskell, K., Hough, P. D., and Swiler, L. P., 2010, DAKOTA, A Multilevel Parallel Object-Oriented Framework for Design Optimization, Parameter Estimation, Uncertainty Quantification, and Sensitivity Analysis, Version 5.0+ User's Manual, SAND2010-2183, Sandia National Laboratories, NM, 368 pp.
- Burruss, R. C., Brennan, S. T., Freeman, P. A., Merrill, M. D., Ruppert, L. F., Becker, M. F., Herkelrath, W. N., Kharaka, Y. K., Neuzil, C. E., Swanson, S. M., Cook, T. A., Klett, T. R., Nelson, P. H., and Schenk, C. J., 2009, Development of a Probabilistic Assessment Methodology for Evaluation of Carbon Dioxide Storage, USGS Open-File Report 2009-1035, 81 pp.
- Class, H., Ebigo, A., Helmig, R., Dahle, H., Nordbotten, J., Celia, M., Audigane, P., Darcis, M., Ennis-King, J., Fan, Y., Flemisch, B., Gasda, S., Jin, M., Krug, S., Labregere, D., Naderi-Beni, A., Pawar, R., Sbai, A., Thomas, S., Trenty, L., and Wei, L., 2009, A benchmark study on problems related to CO<sub>2</sub> storage in geologic formations. *Computers in Geoscience*, 13, 409-434.
- Deutsch, C. V., and Journel, A. G., 1998, GSLIB: Geostatistical Software Library and User's Guide: New York, New York, Oxford University Press, Inc., 369 p.
- EPA, 2010. Overview of Geologic Sequestration.  
[http://www.epa.gov/climatechange/emissions/co2\\_gs\\_tech.html](http://www.epa.gov/climatechange/emissions/co2_gs_tech.html)
- Eldred, M., Giunta, A., van Bloemen Waanders, B., Wojtkiewicz, Jr., S., Hart, W., and Alleva, M., 2002, DAKOTA, A Multilevel Parallel Object-Oriented Framework for Design Optimization, Parameter Estimation, Uncertainty Quantification, and Sensitivity Analysis. Version 3.0 Users Manual, SAND2001-3796. Sandia National Laboratories, Albuquerque, NM.
- European Climate Exchange, 2010. <http://www.ecx.eu/>
- Ghomian, Y., Pope, G. A., and Sephernoori, K., 2008, Reservoir simulation of CO<sub>2</sub> sequestration pilot in Frio brine formation, USA Gulf Coast. *Energy*, 22: 1055-1067.
- GoldSim, 2010. Monte Carlo Simulation Software for Decision and Risk Analysis,  
<http://www.goldsim.com/>
- Helton, J. C., Anderson, D. R., Jow, H.-N., Marietta, M. G., and Basabilvazo G., 1999, Performance assessment in support of the 1996 compliance certification application for the Waste Isolation Pilot Plant, *Risk Analysis*, 19(5): 959-986.

- Holtz, M., Fouad, K., Knox, P., Sakurai, S., and Yeh, J., 2005, Geologic sequestration in saline formations, Frio Brine Storage Pilot Project, Gulf Coast, Texas. DOE/NETL Fourth Annual Conference on Carbon Capture and Sequestration, Paper 240, May 2-5, 2005.
- LeNeveu, D. M., 2008, CQUESTRA, a risk and performance assessment code for geological sequestration of carbon dioxide, Energy Conversion and Management, 49(1): 32-46.
- McKenna, S., 2010. Personal Communication.
- NETL, 2010a. DOE NETL partnerships for carbon sequestration. [http://www.netl.doe.gov/technologies/carbon\\_seq/partnerships/partnerships.html](http://www.netl.doe.gov/technologies/carbon_seq/partnerships/partnerships.html)
- NETL, 2010b. Map of Carbon Storage locations in U.S. [http://www.netl.doe.gov/technologies/carbon\\_seq/refshelf/project%20portfolio/2009/index.html](http://www.netl.doe.gov/technologies/carbon_seq/refshelf/project%20portfolio/2009/index.html)
- NETL, 2010c. U.S. Partners with Canada to Renew Funding for World's Largest International CO<sub>2</sub> Storage Project in Depleted Oil Fields, [http://www.netl.doe.gov/publications/press/2010/PrinterFriendlyHTML\\_1\\_150435\\_150435.html](http://www.netl.doe.gov/publications/press/2010/PrinterFriendlyHTML_1_150435_150435.html). Press Release.
- Oldenburg, C. M., Bryant, S. L., and Nicot, J.-P., 2009, Certification framework based on effective trapping for geologic carbon sequestration, International Journal of Greenhouse Gas Control, 3: 444–457.
- Pruess, K., 2005, ECO2N: A TOUGH2 Fluid Property Module for Mixtures of Water, NaCl, and CO<sub>2</sub>. LBNL-57952. Earth Sciences Division, Lawrence Berkeley National Laboratory, Berkeley, California.
- Pruess, K., Oldenburg, C., and Moridis, G., 1999, TOUGH2 User's Guide, Version 2.0. LBNL-43134. Earth Sciences Division, Lawrence Berkeley National Laboratory, Berkeley, California.
- Quintessa, 2010, CO<sub>2</sub> FEP Database. <http://www.quintessa.org/co2fepdb/PHP/frames.php>. Quintessa Ltd, Oxfordshire, UK.
- Rautman, C. A., and McKenna, S. A., 1997, Three-Dimensional Hydrological and Thermal Property Models of Yucca Mountain, Nevada, Sandia Report SAND97-1730: Sandia National Laboratories, Albuquerque, New Mexico, 322 pp.
- Rish, W. R., 2005. A probabilistic risk assessment of Class I hazardous waste injection sites. In: Tsang, C.-F., Apps, J.A. (Eds.), Underground Injection Science and Technology, 52. Developments in Water Science: 93–125.

- Saadatpoor, E., Bryant, S., and Sephernoori, K., 2007. Effect of heterogeneity in capillary pressure on buoyancy driven flow of CO<sub>2</sub>. DOE/NETL Sixth Annual Conference on Carbon Capture and Sequestration, Pittsburgh, PA, May 7-10, 2007.
- Sasaki, K., Fujii, T., Niibori, Y., Ito, T., and Hashida, T., 2008. Numerical simulation of supercritical CO<sub>2</sub> injection into subsurface rock masses. *Energy Conversion and Management*, 49: 54-61.
- Stauffer, P.H., Viswanathan, H.S., Pawar, R. J., Guthrie, G.D., 2009. A system model for geologic sequestration of carbon dioxide. *Environmental Science and Technology*, 43 (3), 565–570.
- U.S. DOE, 2006. [http://www.fossil.energy.gov/news/techlines/2006/06057-Frio\\_CO2\\_Injection.html](http://www.fossil.energy.gov/news/techlines/2006/06057-Frio_CO2_Injection.html)
- Van Genuchten, M.T., 1980, A closed-form equation for predicting the hydraulic conductivity of unsaturated soils, *Soil Sci. Soc.*, 44, 892-898.
- Viswanathan, H. S., Pawar, R. J., Stauffer, P. H., Kaszuba, J. P., Carey, J. W., Olsen, S. C., Keating, G. N., Kavetski, D., and Guthrie, G. D., 2008, Development of a hybrid process and system model for the assessment of wellbore leakage at a geologic CO<sub>2</sub> sequestration site”, *Environ. Sci. Technol.*, 42 (19), 7280–7286.
- Walton, F. B., Tait, J. C., LeNeveu, D., and Sheppard, M. I., 2005, Geological storage of CO<sub>2</sub>: a statistical approach to assessing performance and risk, In: E.S.Rubin, D.W. Keith and C.F.Gilboy (Eds.), *Proceedings of 7th International Conference on Greenhouse Gas Control Technologies*, Sept 5-9, 2004, Vancouver, Canada. Volume 1: Peer-Reviewed Papers and Plenary Presentations, IEA Greenhouse Gas Programme, Cheltenham, UK, 2004.
- WRI, 2010, Carbon Capture and Sequestration Flow Chart. <http://www.wri.org/chart/carbon-capture-sequestration-flow-chart>

## DISTRIBUTION

1	MS0899	Technical Library	9536 (electronic copy)
1	MS0123	D. Chavez, LDRD Office	1011

